CHAPTER 4

RESULTS AND DISCUSSION

4.1 Modeling results for dragline boom

The three dimensional model of dragline boom has been constructed in SolidWorks using the dimensions and specifications of boom as tabulated in table no 3.1 as described in research methodology chapter. The global beam model for static loading conditions created in SolidWorks is shown in figure 4.1. The constructed model has fairly simplified the preparation of dragline boom for its critical analysis. However, the design prepared in SolidWorks cannot be directly imported in ANSYS. Therefore, the wireframe file was converted to IGES file format, which was then imported to ANSYS workbench for defining cross sections and other relevant dimensions for its critical analysis.

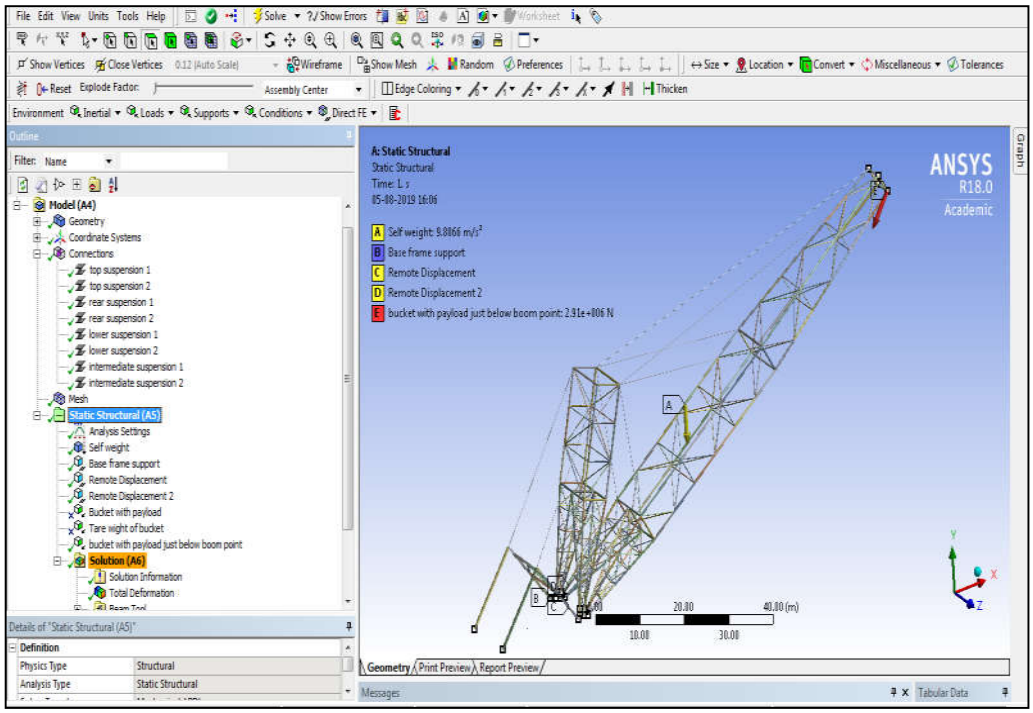

Figure 4.1 Global beam model of dragline boom

The construction of dragline boom has been able to provide a perfect visualization of the boom in three dimensions (3D). SolidWorks proves to be an effective tool for construction of 3D models for complex structure and any change in design parameters incorporated during any phase of the design gets automatically updated for the entire structure without redrawing from the scratch at each and every time. A number of SolidWorks tools were used for the creation of drawing layout to accurately represent the dragline model.

4.2 Stress analysis of the dragline boom

The stress analysis has been done under static and dynamic loading conditions of the dragline boom as discussed in the following section.

4.3 Stress analysis of the dragline boom under static loading condition

Bucket with payload case is considered only at boom point in a global beam model. Boom loading under different ratio of the hoist rope and drag rope will put the boom under different loading conditions during digging operation. Its repeated nature can accelerate fatigue. However, a fixed ratio will induce static load for a certain time.

4.3.1 Boom under self- weight condition

Boom under self-weight condition implies that only the dead load of the boom has been applied in the analysis. Dragline booms are made up of hollow circular steel pipes having density between 7800-8000 kg/m^3. In the current analysis the weight of the boom has been computed as 140 ton from the constructed model. Based on the computed self-weight the deformation, Von-Mises stresses fatigue life, and factor of

safety (FOS) results have been obtained for the boom structure, from the constructed global beam and solid submodel.

a) Global beam model results for dragline

The results have been tabulated in table 4.1 and figure 4.2 displays the global beam model results for the entire structure under self-weight condition of the boom. Total deformation has been found as 341 mm at the top most point of the boom as revealed in red color in figure 4.2(a). Direct stress was found to be maximum at A-frame rear members with a value of 33.42 MPa (tensile), while the maximum value in compression for direct stresses at mast was found to be 77 MPa (figure 4.2 (b)). Maximum bending stress was found to be 113 MPa at the point of attachment of suspension rope connecting mast with the boom as illustrated in figure 4.2 (c). Value of maximum combined stresses for the entire structure, which is the sum of direct stress and bending stress found at a particular point are depicted in figure 4.2(d). These can be tensile or compressive in nature. For the given self-weight loading condition, these stresses have been obtained as 134.38 MPa in tensile and 76 MPa in compression.

Table 4.1 Self-weight loading case of global beam model

Load Case	**Deformation (m)**	**Direct Stress (MPa)**		**Maximum Bending Stress (MPa)**		**Combined Stress (MPa)**	
Boom under self-weight		Compression	77.69	Max.	113.18	Compression	74.62
	0.3416						
		Tension	33.42	Min.	1.74 x e-4	Tension	134.38

Global beam model 4.2 (a-d) clearly suggest that dragline boom suffers maximum deformation caused by the large self- weight of the boom itself. The gravity load generates stresses within the entire structure, commonly known as direct stresses. The red and blue color shows the maximum and minimum values respectively. Bending stress is also generated by the application of gravity load, as the load is not parallel to the plane of the boom. The brace members are subjected to most of the bending stress and prevent the excessive deformation of structure due to applied load.

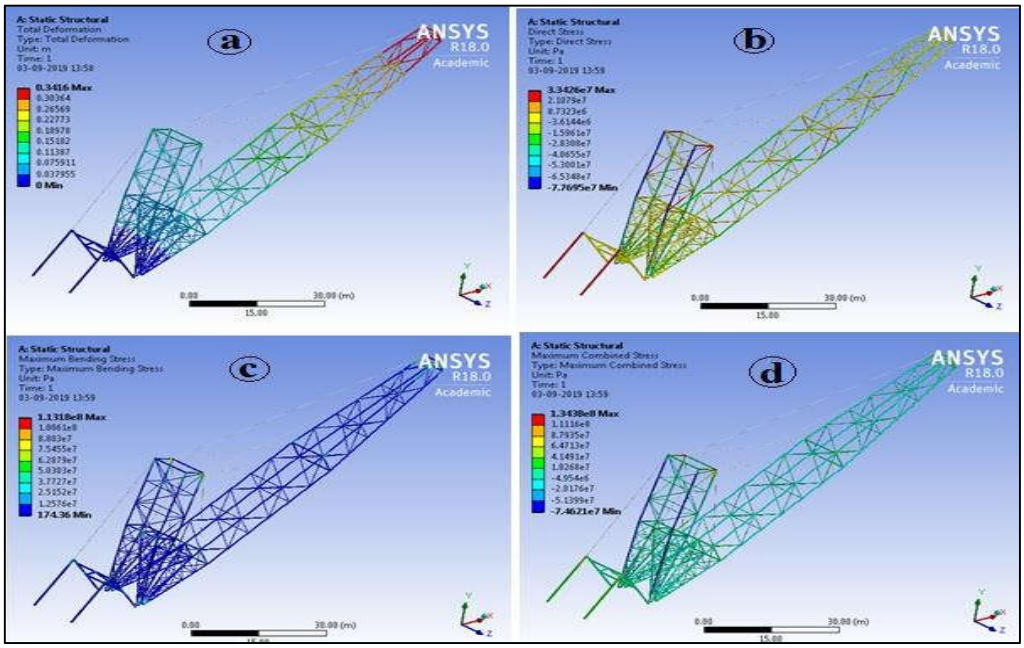

Figure 4.2 Global beam model results for a) deformation, b) axial stress c) maximum bending stress and d) maximum combined stress

b) Equivalent stress (Von-Mises) on dragline boom under self-weight

The equivalent stress distribution has been shown in the figure 4.3 (a-d). The analysis of equivalent stress (Von-Misses) reveals that due to self-weight of the boom, the maximum equivalent stresses occur in the vicinity of the brace- chord intersection point. The Von-Mises stress reaches maximum value of 75.51 MPa at

the joint location 2. Joint 1 and joint 3 have the stress value of 45.87 MPa and 42.57 MPa respectively. For joint 4 stresses value has been found to be 52.59 MPa.

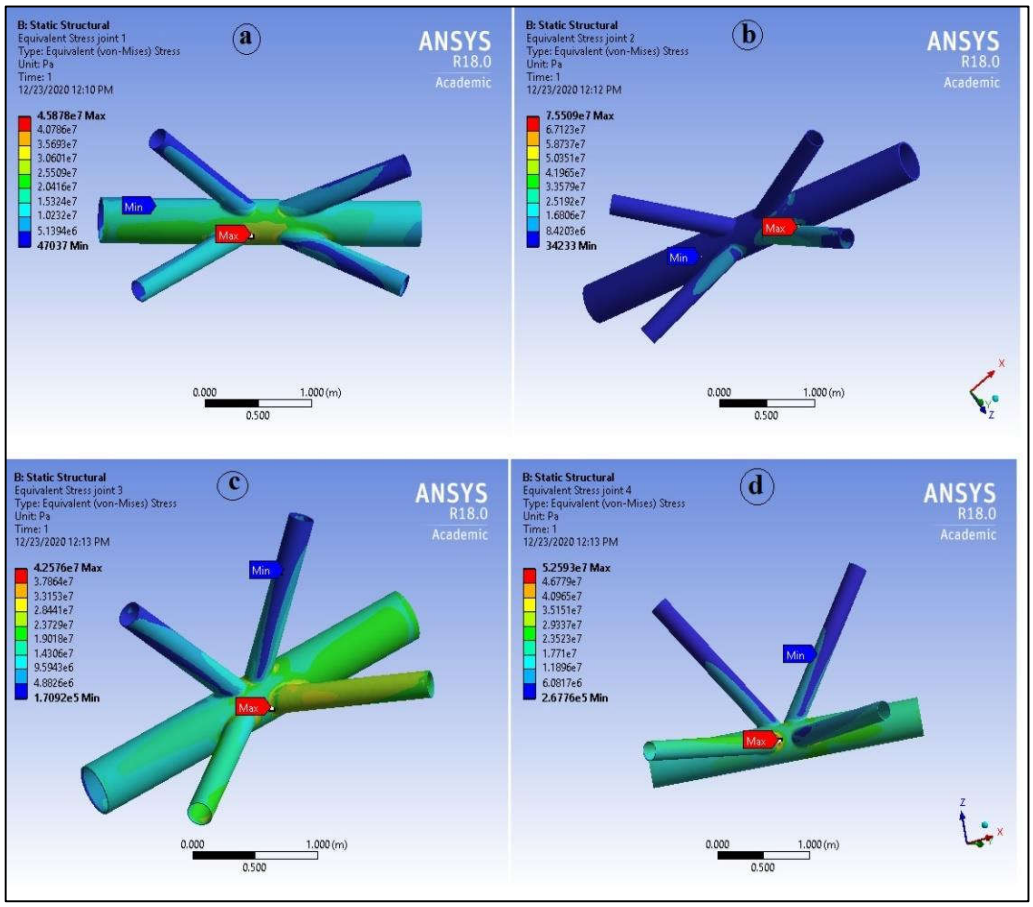

Figure 4.3 Equivalent stresses (Von-Mises) stress distribution for four selected joints

The Von-Mises stresses are high at joint 2 and joint 4 owing to their nearness of the joints to boom point sheave and boom foot. On the other hand, stress on joint 1 and joint 3 are comparatively lower. This confirms the hypothesis of joint selection for analysis.

The results of the observed value have been tabulated in table 4.2

Table 4.2 Equivalent stress results of critical joints

Load Case	Type of result	Joint 1	Joint 2	Joint 3	Joint 4
Boom under self-weight	Equivalent stress (MPa)	45.87	75.51	42.57	52.59

c) Fatigue life of joints under self-weight of boom

For fatigue life analysis of the selected joints, the self-weight of the structure has been assumed to be acting at a point, which is considered as the center of gravity of the entire boom structure. In the analysis as stresses in all the joints are below the value of endurance limit of the structural steel. The stresses below endurance limit of the material clearly imply no fatigue failure in the components. The fatigue life has been tested for 1 x e6 no of iterations as obtained for all the location (figure 4.4 a-d).

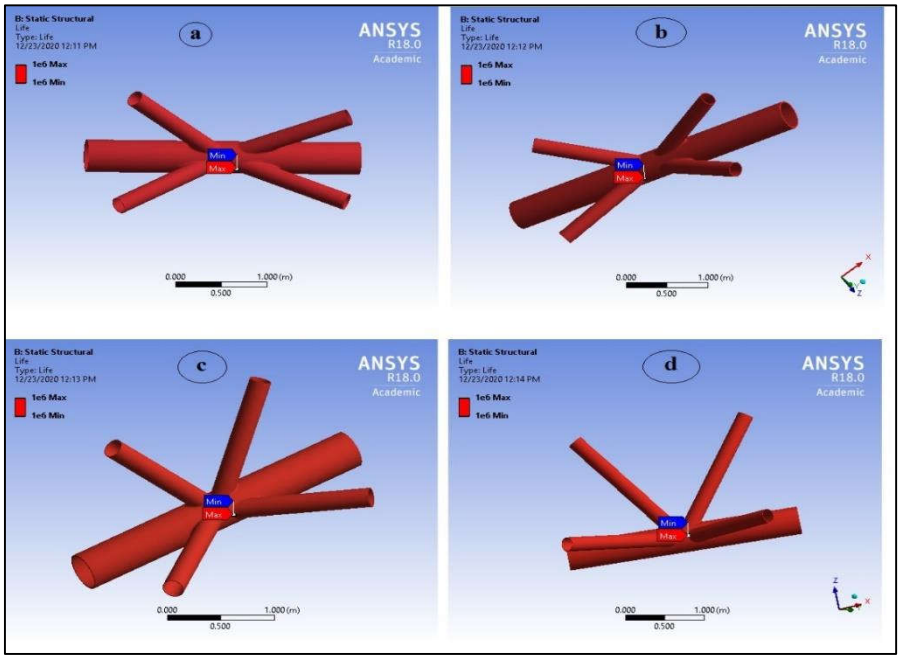

Figure 4.4 Fatigue life results for selected locations

The results of the observed value have been tabulated in table 4.3.

Table 4.3 Fatigue life results for critical joint locations

STATIC ANALYSIS RESULTS FOR SELECTED LOCATIONS					
Load Case	**Type of result**	**Joint 1**	**Joint 2**	**Joint 3**	**Joint 4**
Boom under self-weight	Fatigue life (number of cycles)	1 x e6	1 x e6	1 x e6	1 x e6

d) Factor of safety (FOS)

Based on the fatigue life and damage in the components, factor of safety has also been also computed. The FOS has been assessed on the scale ranging from zero to fifteen (standard practice in ANSYS workbench static structural module). A value of fifteen ensures the maximum life at selected locations without failure and safety factor magnitude below one indicates the probability of first crack in the component. The minimum factor of safety has been found to be 2.20 at joint Location 2 as shown in figure 4.5(b). For other three joints under consideration 1,3 and 4 the value of safety factor was found to be 3.63, 3.91 and 3.17 respectively as shown in figure 4.5 (a, c and d). As such, the designed model appears to be fairly safe and conservative from the fatigue failure. The results of the observed value have been tabulated in table 4.4 and shown in figure 4.5.

Table 4.4 Factor of safety results for critical joints

STATIC ANALYSIS RESULTS FOR SELECTED LOCATIONS					
Load Case	**Type of result**	**Joint 1**	**Joint 2**	**Joint 3**	**Joint 4**

Boom under self-weight	Factor of safety (FOS)	3.63	2.20	3.91	3.17

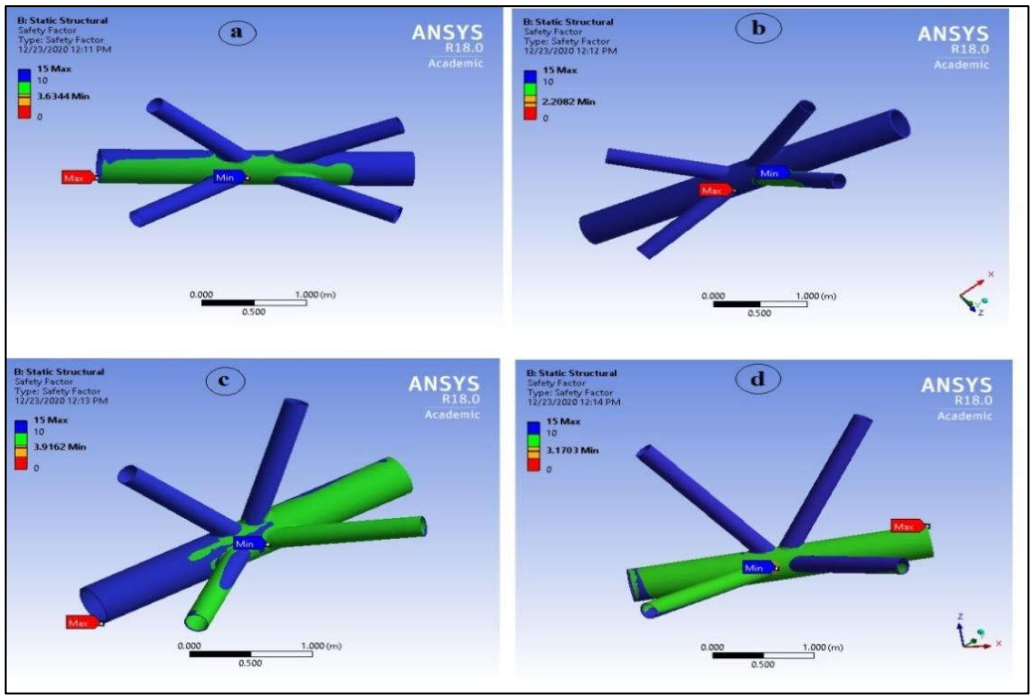

Figure 4.5 Fatigue based FOS for selected joint locations

4.3.2 Analysis of self-weight of boom along with the empty bucket acting on boom

Dragline bucket is directly attached to the dragline boom by means of hoist ropes. The self-weight of empty bucket is transferred from these ropes to the dragline boom. In the current case bucket self-weight (tare weight) is additionally considered in conjunction with the self-weight of boom.

a) Global beam model results for dragline

The tare weight of bucket has been established as 26 ton (as computed in research and methodology chapter no 3), which increases the value of deformation for the

entire boom structure, as the load is directly transferred to the boom by hoist ropes. The magnitude of deformation in this case has been found as 476 mm in comparison to 341 mm observed in the previous case. Similarly, the magnitude of the direct stresses has been obtained as 104.65 MPa in compression and 47.12 MPa in tension in comparison to 77 MPa and 33 MPa respectively in the self- weight case as shown in figure 4.6 (b). Maximum bending stress was found to be 110.62 MPa at the point of attachment of suspension rope connecting mast with the boom as illustrated in figure 4.6 (c). The value of maximum combined stress was 149.15 (tensile) and 100.48 MPa (compressive) were obtained as shown in figure 4.6 (d) in a color range between blue (compressive) and red (tensile).

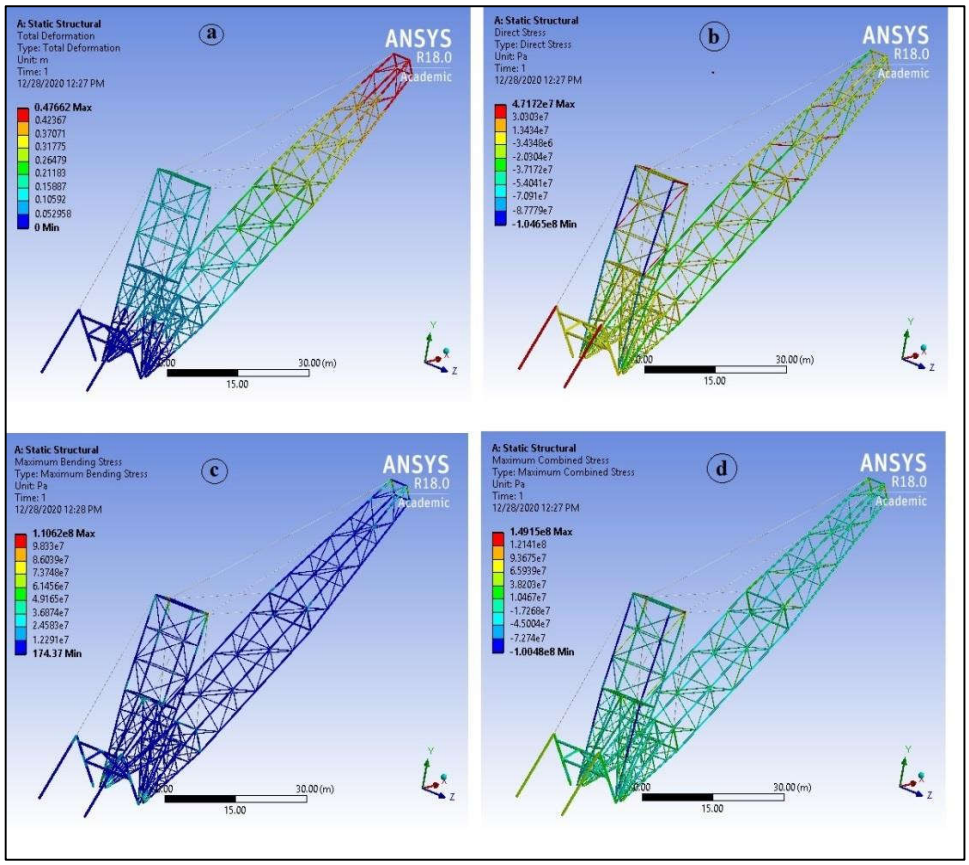

Figure 4.6 Global beam model results for (a) deformation, (b) axial stress (c) maximum bending stress and (d) maximum combined stress

The results of the observed value has been tabulated in table 4.5

Table 4.5: Self-weight loading case of global beam model

STATIC ANALYSIS RESULTS FOR GLOBAL BEAM MODEL							
Load Case	**Deformation (m)**	**Direct Stress (MPa)**		**Maximum Bending Stress (MPa)**		**Combined Stress (MPa)**	
Boom under self-weight and tare weight of bucket		Compression	104.65	Max.	110.62	Compression	100.48
	0.476						
		Tension	47.17	Min.	1.74 x e-4	Tension	149.15

b) Equivalent stress (Von-Mises stress) of dragline boom

As shown in figure 4.7 (a-d) and tabulated in table 4.6, stresses at joint location 2 rises rapidly up to 98.78 MPa, while the stress value for joint location 1 reached to 86.43 MPa. As Joint 1 and 2 were near to the load application point and therefore they suffer higher loading as compared to the other two joints chosen for the analysis. The value of equivalent Von- Mises stress for other two joints 3 and 4 was computed as 65.38 MPa and 62.74 MPa respectively.

Table 4.6 Equivalent stress results of critical joints

STATIC ANALYSIS RESULTS FOR SELECTED LOCATIONS					
Load Case	**Type of result**	**Joint 1**	**Joint 2**	**Joint 3**	**Joint 4**

`Boom under self-weight and tare weight of bucket	Equivalent stress (MPa)	86.43	98.78	65.38	62.74

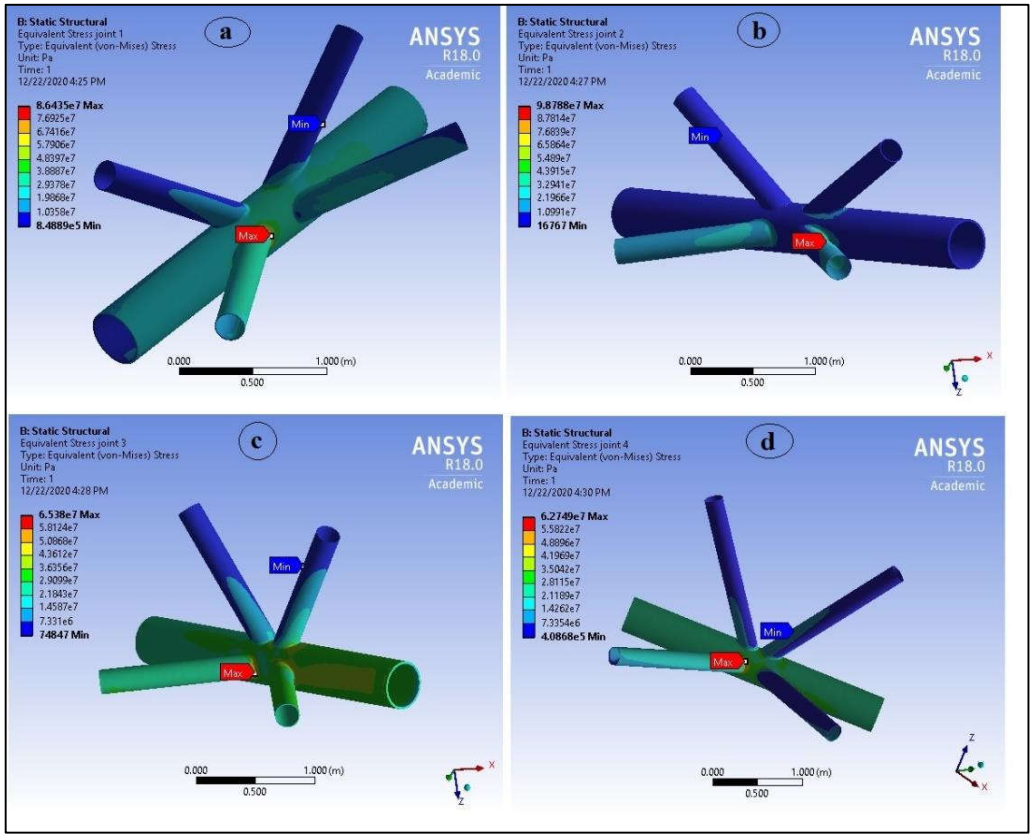

Figure 4.7 Equivalent stresses (Von-Mises) stress distribution for four selected joints

c) Fatigue life

Fatigue failure is particularly insidious because it occurs without any obvious warning. For all Joints under consideration, fatigue life of $1xe^6$ cycles was obtained as revealed in figure 4.8 (a-d). It is clearly observed that that the stress magnitudes affect fatigue life. Furthermore, the fatigue strength is seriously reduced by the introduction of stress elevators such as, a notch or hole. One of the best ways of

minimizing fatigue failure is by the reduction of avoidable stress elevators through careful design and the prevention of accidental stress elevators by careful machining and fabrication.

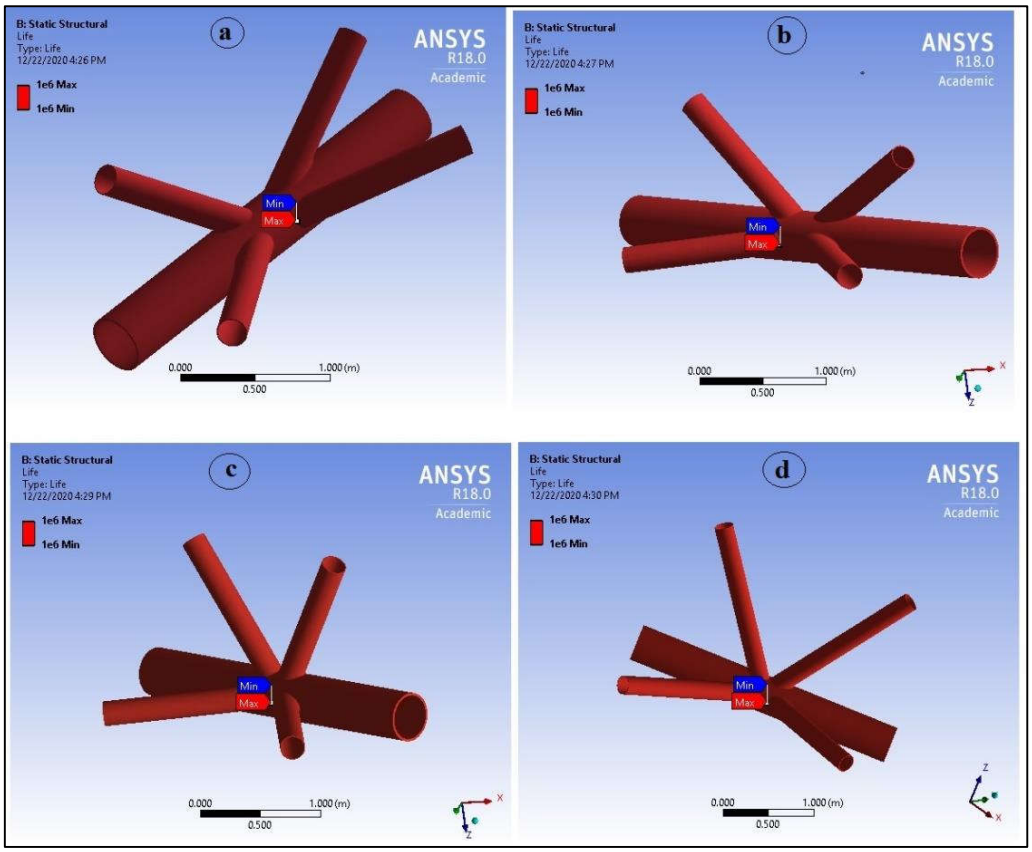

Figure 4.8 Fatigue life results for selected locations

The results of the observed value has been tabulated in table 4.7

Table 4.7: Fatigue life results for critical joints

STATIC ANALYSIS RESULTS FOR SELECTED LOCATIONS					
Load Case	**Type of result**	**Joint 1**	**Joint 2**	**Joint 3**	**Joint 4**

Boom under self-weight and tare weight of bucket	Fatigue life (number of cycles)	1 x e6	1 x e6	1 x e6	1 x e6

d) Factor of safety (FOS)

Factor of safety is a contour plot with respect to fatigue failure at a given design life. It has been observed from the analysis that the factor of safety is minimum near brace –chord intersection point for joint 2 as seen in figure 4.9(a-d). The minimum value of factor of safety is 1.68 near the brace chord intersection point for joint 2. The remaining of the joints have higher values. Being subjected to high stress values the factor of safety has been observed to be low in these joints of the dragline boom.

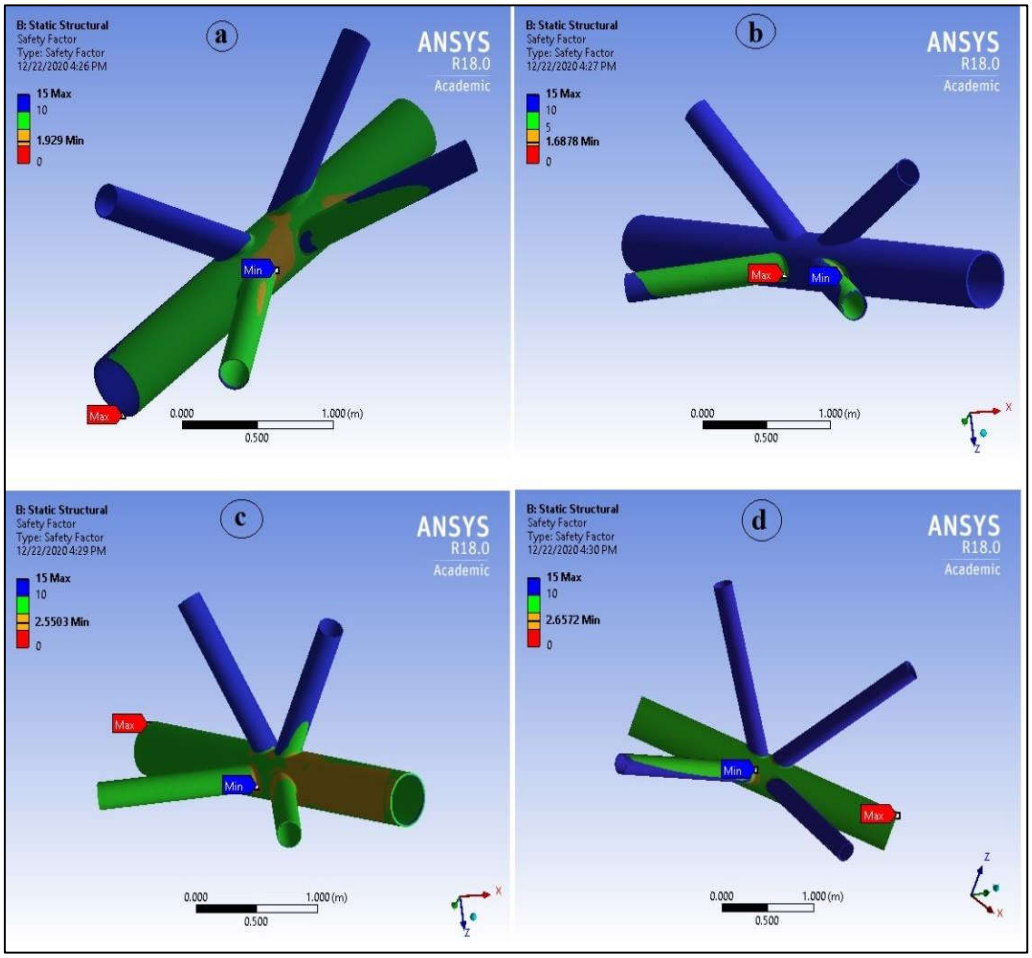

Figure 4.9 Factor of safety for selected joint locations

The results of the observed value has been tabulated in table 4.8

Table 4.8: Factor of safety results for critical joints

STATIC ANALYSIS RESULTS FOR SELECTED LOCATIONS					
Load Case	**Type of result**	**Joint 1**	**Joint 2**	**Joint 3**	**Joint 4**
Boom under self-weight and tare weight of bucket	Factor of safety (FOS)	1.93	1.68	2.55	2.65

4.3.3 Bucket with payload below boom point

The boom in loaded condition means that dead load of boom and bucket plus payload acting on the boom has been used in the analysis, and the value of the payload has been computed as 6.15 x10^5 N for broken sandstone material (computed in research and methodology chapter). This load has been applied on the boom directly. By applying the boundary and loading conditions, the results have been obtained for stress, damage, fatigue life, factor of safety and fatigue sensitivity as discussed in following sections.

a) Global beam model based results for dragline boom

Application of payload along with dead load of bucket and boom further increase the stress on the dragline boom. Deformation value has been increased up to 656 mm for the structure with its maximum value at boom upper region depicted in figure 4.10(a). The values of direct stresses have been obtained as 140.57 MPa in compression and 69.15 MPa in tension as revealed in figure 4.10(b). The value of bending stress also increases and reaches up to 116 MPa, while maximum combined stresses reaches in the range of 135.02 MPa (compression) to 168.83 Mpa (tension) as depicted in figure 4.10(c), (d) respectively.

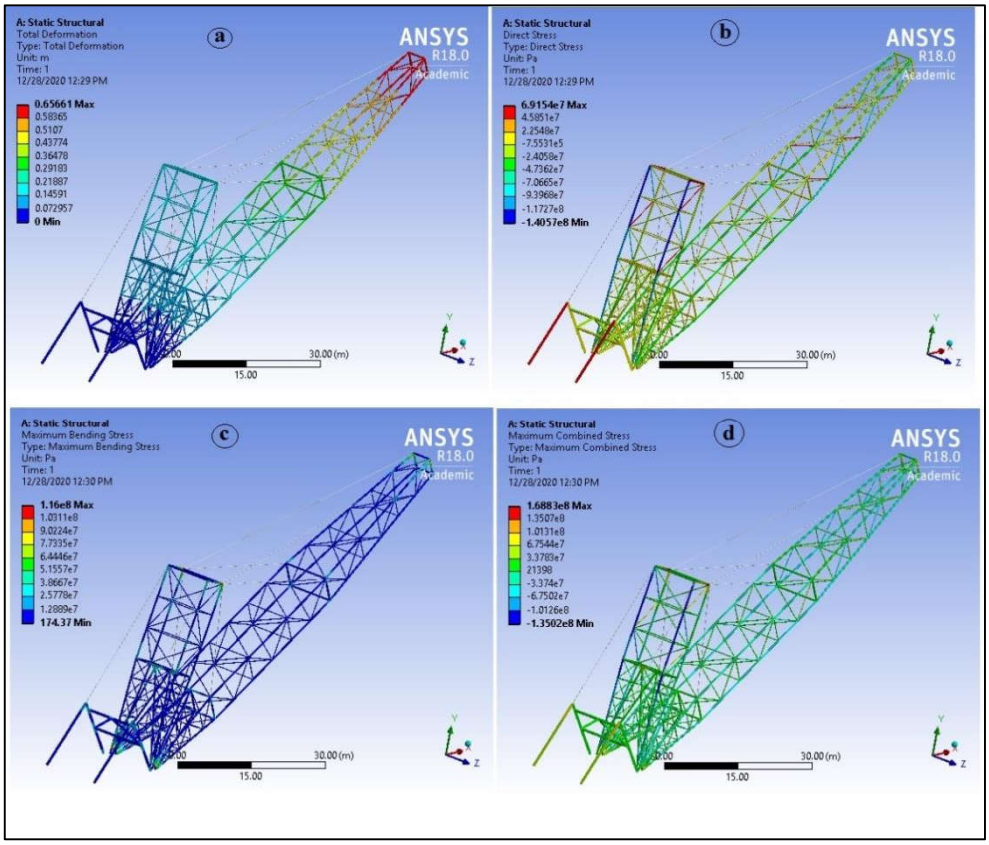

Figure 4.10 Global beam model results for a) deformation, b) axial stress c) maximum bending stress and d) maximum combined stress

The results of the observed value have been tabulated in table 4.9.

Table 4.9: Static analysis results for global beam model

STATIC ANALYSIS RESULTS FOR GLOBAL BEAM MODEL							
Load Case	**Deformation (m)**	**Direct Stress (MPa)**		**Maximum Bending Stress (MPa)**		**Combined Stress (MPa)**	
Boom with bucket payload along with above loadings		Compression	140.57	Max.	116.00	Compression	168.83
	0.656						
		Tension	69.15	Min.	1.74 x e-4	Tension	135.02

b) Equivalent stress (Von-Mises) of dragline boom

As clearly illustrated in figure 4.11 (a-d) the equivalent stresses value for all four joints is below the yield strength of material (250 MPa for steel). Joint 2, which is near to the load application point shows the stress value of 123.05 MPa, while joint 1 has the stress value of 133.48 MPa. In this case the joint 3 has also been severely affected by the load application and has thus resulted in a sharp increase in stress level with value of 99.37 MPa. However joint 4, which is far enough from the load application region do not show such phenomena and a very small increment in stress (65.56 MPa) has been observed.

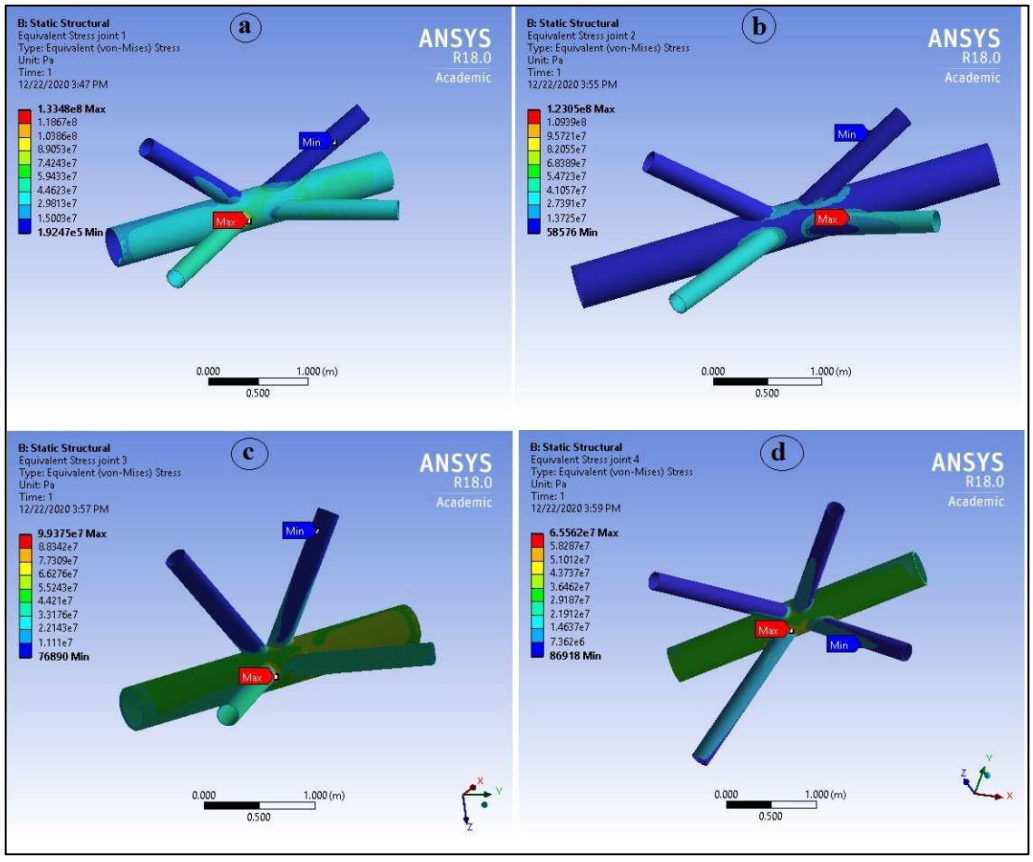

Figure 4.11 Equivalent stresses (Von-Mises) stress distribution for four selected joints

The results of the observed value has been tabulated in table 4.10

Table 4.10 Equivalent stress results of critical joints

STATIC ANALYSIS RESULTS FOR SELECTED LOCATIONS					
Load Case	**Type of result**	**Joint 1**	**Joint 2**	**Joint 3**	**Joint 4**
`Boom under self-weight along with tare and payload of bucket	Equivalent stress (MPa)	133.48	123.05	99.37	65.56

c) Fatigue life

The increased value of stress for the joints further reduced the fatigue life. Although the loading is high enough to increase the stress value, but none of the joints are stressed beyond the yield strength of the material. Maximum design life has been obtained for all the joints as clearly depicted in figure 4.12 (a-d) and tabulated in table 4.11.

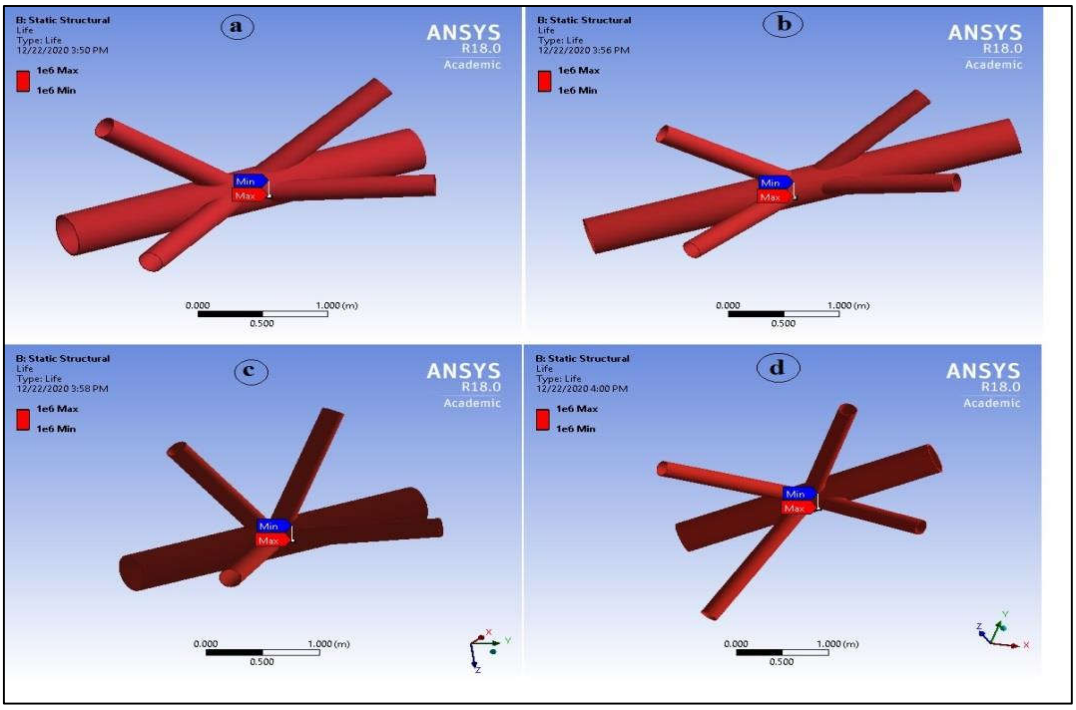

Figure 4.12 Fatigue life results for selected locations

Table 4.11: Fatigue life results for critical joints

STATIC ANALYSIS RESULTS FOR SELECTED LOCATIONS					
Load Case	**Type of result**	**Joint 1**	**Joint 2**	**Joint 3**	**Joint 4**
Boom under self-weight along with tare and payload of bucket	Fatigue life (number of cycles)	1 x e6	1 x e6	1 x e6	1 x e6

d) Factor of safety (FOS)

Factor of safety for all the joints has been reduced significantly in comparison to previous case and found to be lowest for joint 1 as shown in figure 4.13. The value of the factor of safety for joint 2 has been observed as 1.35. Factor of safety less than 1 indicates that material exceeds elastic limit and if it is greater than 1, it indicates that it works without problem. In this case, the analysis reveals that the minimum value of factor of safety is 1.25 for joint 1.

The factor of safety values are tabulated in table 4.12. From the results of FOS values it is quite evident that the joint 1 has the lowest FOS and joint 4 has the highest value.

Table 4.12: Factor of safety results for critical joints

STATIC ANALYSIS RESULTS FOR SELECTED LOCATIONS					
Load Case	**Type of result**	**Joint 1**	**Joint 2**	**Joint 3**	**Joint 4**
Boom under self-weight along with tare and payload of bucket	Factor of safety (FOS)	1.24	1.35	1.68	2.54

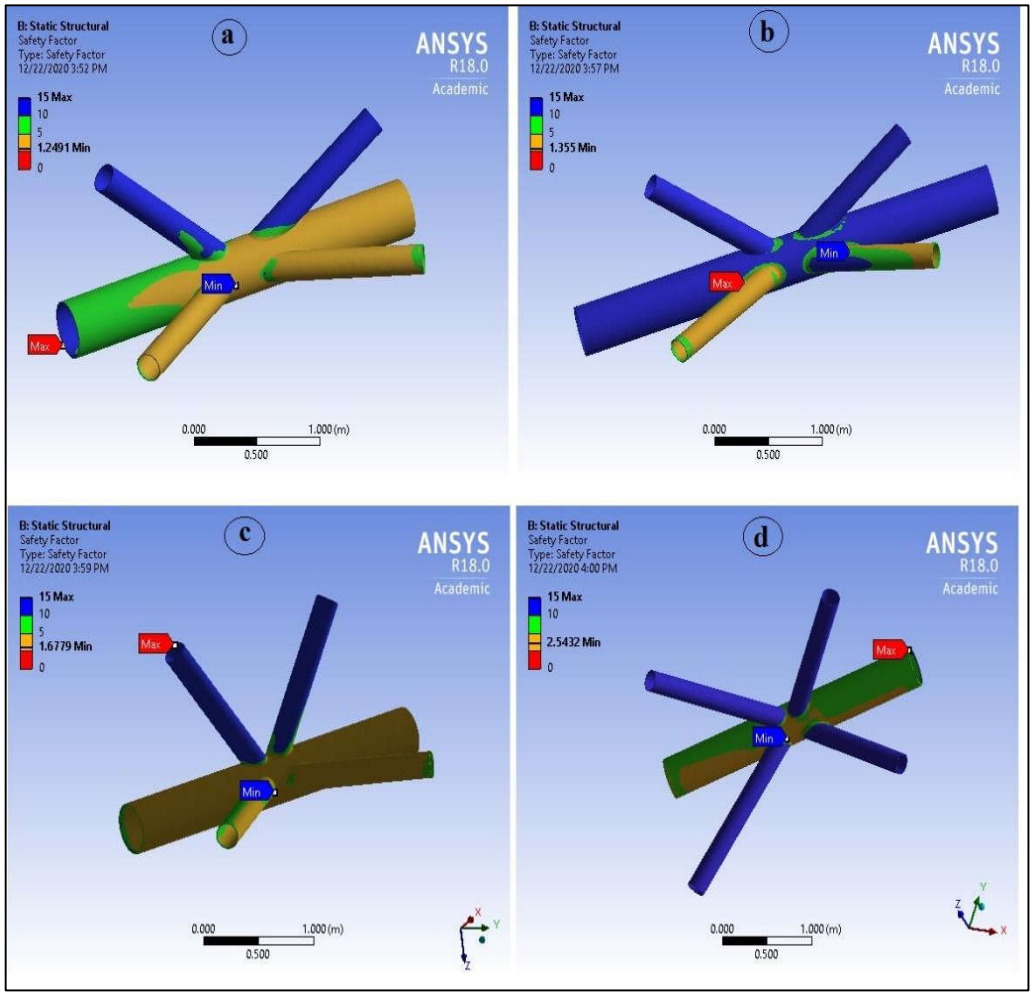

Figure 4.13 Factor of safety for selected joint locations

4.4 Summary of the static load cases

The results from the above three static load cases are tabulated in table 4.13 and table 4.14. Table 4.13 enlist the observations from global beam model, which gives sufficient information about the deformation of the structure, direct stress in members, bending stresses and maximum combined stresses. It helps in identifying the critical areas (selection of critical joints) of the structure for further detailed analysis of Von-Mises stress, fatigue life, factor of safety.

Table 4.13: Comparative Static analysis results for various study cases of global beam model

STATIC ANALYSIS RESULTS FOR GLOBAL BEAM MODEL							
Load Case	**Deformation (m)**	**Direct Stress (MPa)**		**Maximum Bending Stress (MPa)**		**Combined Stress (MPa)**	
Boom under self-weight		Compression	77.69	Max.	113.18	Compression	74.62
	0.3416						
		Tension	33.42	Min.	1.74 x e-4	Tension	134.38
Boom under self-weight and tare weight of bucket		Compression	104.65	Max.	110.62	Compression	100.48
	0.476						
		Tension	47.17	Min.	1.74 x e-4	Tension	149.15
Boom with bucket payload along with above loadings		Compression	140.57	Max.	116.00	Compression	168.83
	0.656						
		Tension	69.15	Min.	1.74 x e-4	Tension	135.02

In case of bucket weight with payload, the center of gravity of the entire structure is changed as compared to boom under self-weight. The deformation is increased from 341 mm to 656 mm from self-weight condition to payload condition. The finding confirms that increase in load on boom increases the deformation value. Combined stresses call for further analysis of the structure, as it states about the compressive or tensile behavior at particular point. The compression value for combined stresses has been observed higher in case of payload condition as compared to self-weight condition.

Table 4.14: Comparative Static analysis results for various study cases of solid sub-model

STATIC ANALYSIS RESULTS FOR SELECTED LOCATIONS						
Load Case	**Sr. No.**	**Type of result**	**Joint 1**	**Joint 2**	**Joint 3**	**Joint 4**
Boom under self-weight	1.	Equivalent stress (MPa)	45.87	75.51	42.57	52.59
	2.	Fatigue life (number of cycles)	1 x e6	1 x e6	1 x e6	1 x e6
	3.	Factor of safety (FOS)	3.63	2.20	3.91	3.17
Boom under self-weight and tare weight of bucket	1.	Equivalent stress (MPa)	86.43	98.78	65.38	62.74
	2.	Fatigue life (number of cycles)	1 x e6	1 x e6	1 x e6	1 x e6
	3.	Factor of safety (FOS)	1.93	1.68	2.55	2.65
Boom under self-weight along with tare and payload of bucket	1.	Equivalent stress (MPa)	133.48	123.05	99.37	65.56
	2.	Fatigue life (number of cycles)	1 x e6	1 x e6	1 x e6	1 x e6
	3.	Factor of safety (FOS)	1.24	1.35	1.68	2.54

Table 4.14 enlisted the observations of four critical joints of the boom for different loading cases. The stress values increase in the joint fillet region with the increased loading. Equivalent stresses were found to be increased from 45.87 MPa in self-weight case to 133.48 MPa in payload condition. All the selected joints were having stressed level below their endurance limit. Safety factor of the joint 1 under the self-weight with bucket weight and payload has been obtained as 1.24, which although safe, has the least FOS. Therefore, it may be inferred that the joints have been

designed satisfactorily. However, the probability of failure at this joint location is higher as compared to other joints and it needs to be carefully monitored in real time operation.

4.5 Fatigue sensitivity of dragline boom joint

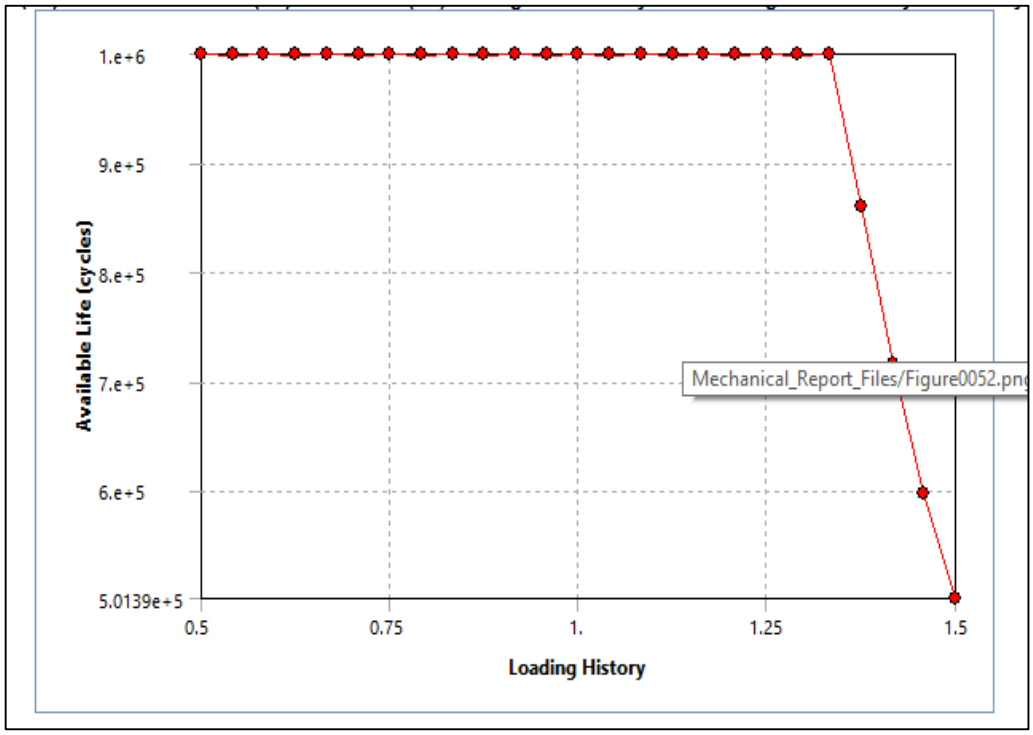

Figure 4.14 Fatigue sensitivity of joint 1under static loading condition (maximum loading)

Figure 4.14 shows the fatigue sensitivity curve for the identified critical joint 1 with FOS 1.24. Fatigue sensitivity shows that how the fatigue results change as a function of loading at the critical location in the model. In the present study, joint number 1 appears to be the most critical location on the boom structure during digging with the maximum loading condition.

The fatigue sensitivity curve for this joint shows that if the static loading is lowered to 50% of its magnitude, life of the joint will increase to the maximum life (1x e6).

On the contrary if its magnitude increases to 150%, then life of the joint decreases. The static loading magnitude, for the study dragline, of 100 % represents the real time loading situation

4.6 Dynamic loading condition analysis of dragline boom

The dynamic loading condition exists during swing –to and swing-back segment of the dragline cycles. This dynamic swinging of the boom will create additional stresses on the dragline boom. The maximum dynamic load is directly related to the maximum swing acceleration and maximum swing velocity. The computation of velocity and accelerations during the swing segments have been clearly explained in research methodology chapter.

For average swing angle of 90^0, the average swing to time was recorded in the field as 21 sec. and average swing back time was about 20 sec. Almost all the dragline studied in the field conformed to this time range and satisfy the regression equation as discussed in chapter 3. Assuming the acceleration phase for the dragline about 16 seconds and constant angular acceleration value of about 0.36 degree / sec^2, the maximum angular velocity obtained after 16 seconds is 6 degree/ sec. The data was rigorously gathered during the field visits and observation.

Therefore, in the computations the maximum angular velocity of dragline boom has been taken as 6 degree/ sec and acceleration value of about 0.36 degree/sec^2.

4.6.1 Boom swing to motion with bucket payload

a) Global beam model

During the dragline operation, after filling the material in the bucket, the dragline used to swing counter clockwise to the disposal site. The rotation of the upper house

of the machinery was performed by providing swing acceleration in the counter clock wise direction. Thus, the rotational inertia creates an additional stresses on the entire structure along with self-weight of the boom, tare and payload weight of the bucket. Given this, it has been found that the deformation value in the boom structure reaches up to 683 mm attaining this maximum value at the tip of the boom. In figure 4.15 (a), the tip of the boom is depicted in red color showing maximum deformation. Direct stress ranged from 135.72 MPa in compression to 76.26 MPa in tension (figure 4.15 (b)). Maximum bending stress has been found to be 114.5 MPa, while maximum combined stress value was computed as 174.3 MPa in tension and 134.56 MPa in compression as illustrated in figure 4.15 (c, d).

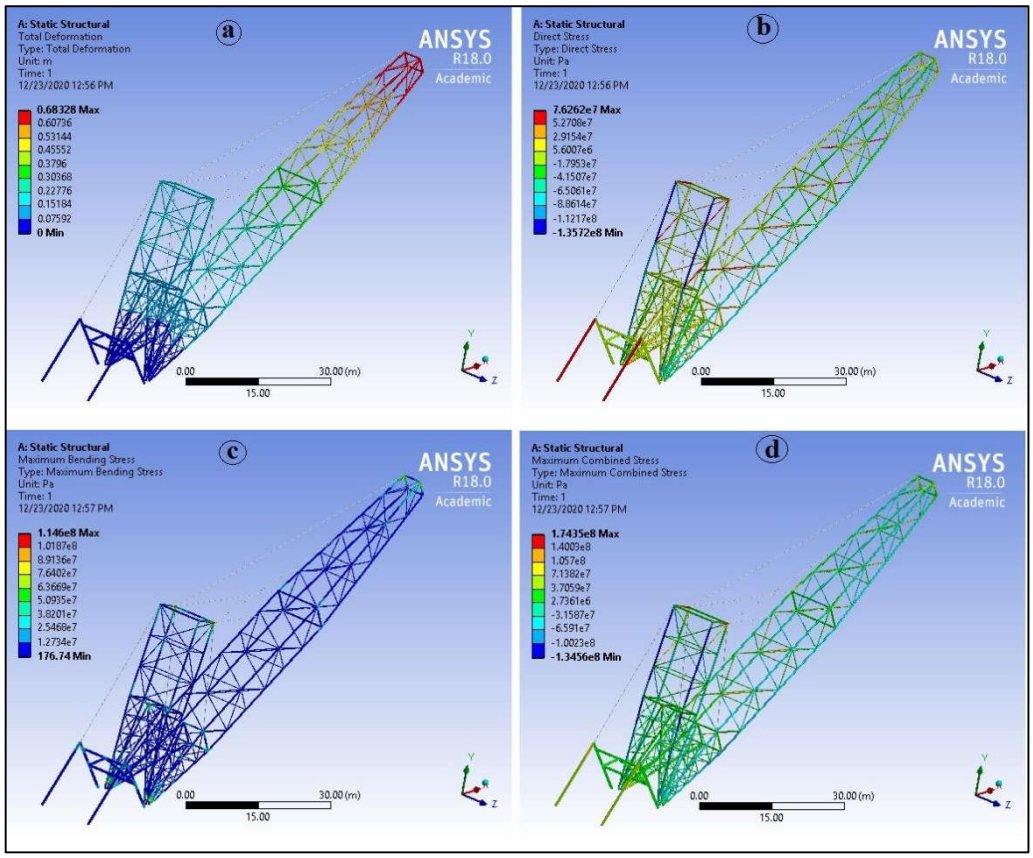

Figure 4.15 Global beam model results for a) deformation, b) axial stress c) maximum bending stress and d) maximum combined stress

The results of the observed value has been tabulated in table 4.15

Table 4.15: Results for global beam model

DYNAMIC ANALYSIS RESULTS FOR GLOBAL BEAM MODEL							
Load Case	**Deformation (m)**	**Direct Stress (MPa)**		**Maximum Bending Stress (MPa)**		**Combined Stress (MPa)**	
Boom swing to motion		Compression	135.72	Max.	114.60	Compression	134.56
	0.683						
		Tension	76.26	Min.	1.76 x e-4	Tension	174.35

b) Equivalent stress (Von-Mises) on boom

The Von-Mises stress values have been found as shown in figure 4.16(a-d) and tabulated in table 4.16. Joint 3 has highest amount of stresses ranging from 1.75 MPa to 142.17 MPa. The stress value is well below the yield strength of the material which is 250 MPa. This amount of stress is not enough to cause fatigue failure of the dragline boom joint at this location. For joint locations 1, 2 and 4 the maximum stress value has been computed as 106.96 MPa, 132.96 MPa and 128.91 MPa respectively.

Table 4.16:Equivalent stress results of critical joints

DYNAMIC ANALYSIS RESULTS FOR SELECTED JOINT LOCATIONS					
Load Case	**Type of result**	**Joint 1**	**Joint 2**	**Joint 3**	**Joint 4**
Boom swing to	Equivalent stress (MPa)	106.96	132.96	142.17	128.91

motion					

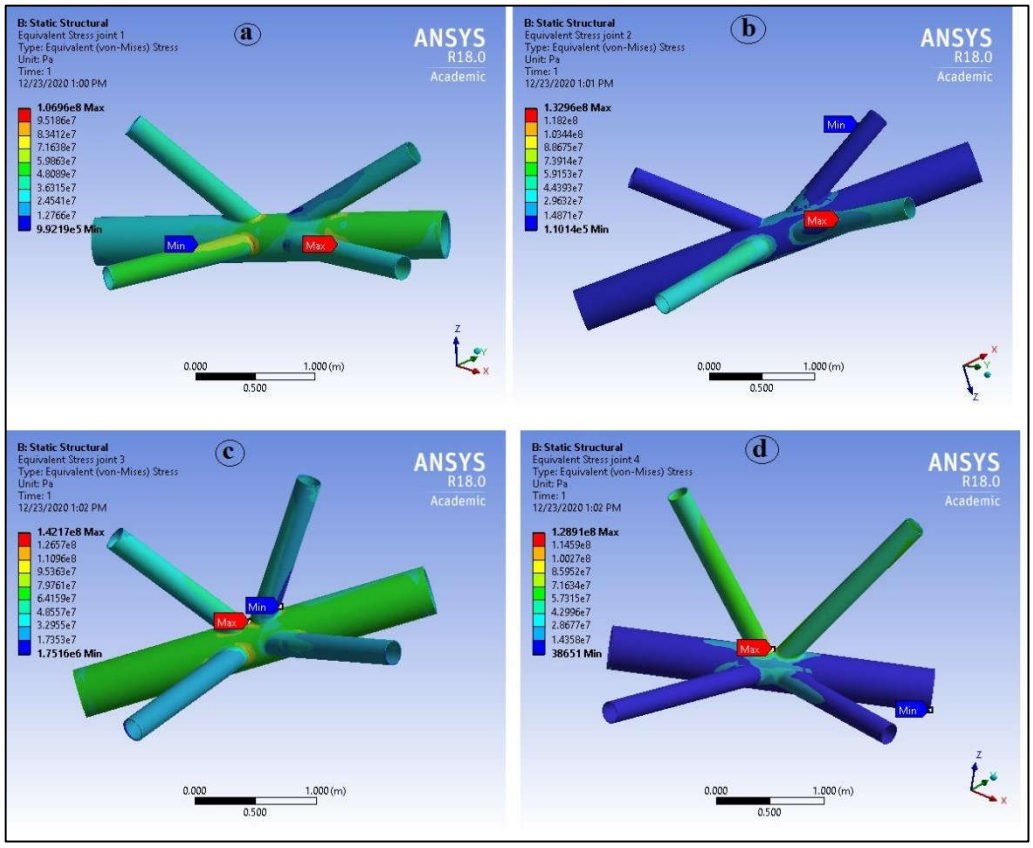

Figure 4.16 Equivalent stress (Von-Mises) stress distribution for four selected joints

The results of the observed value have been tabulated in table

c) Fatigue life

Fatigue results clearly indicate that joint number 3 in this case become important from analysis point of view. The distance of this joint from revolving center and its strategic location near center of gravity of the structure makes it highly stressed. However the stresses at this level are not enough to cause decrease in fatigue life. The fatigue life for all the four locations were found to be 1 x e^6 no of cycles, which

means the joint will certainly going to complete its design life as illustrated in figure 4.17 (a-d) and tabulated in table 4.17.

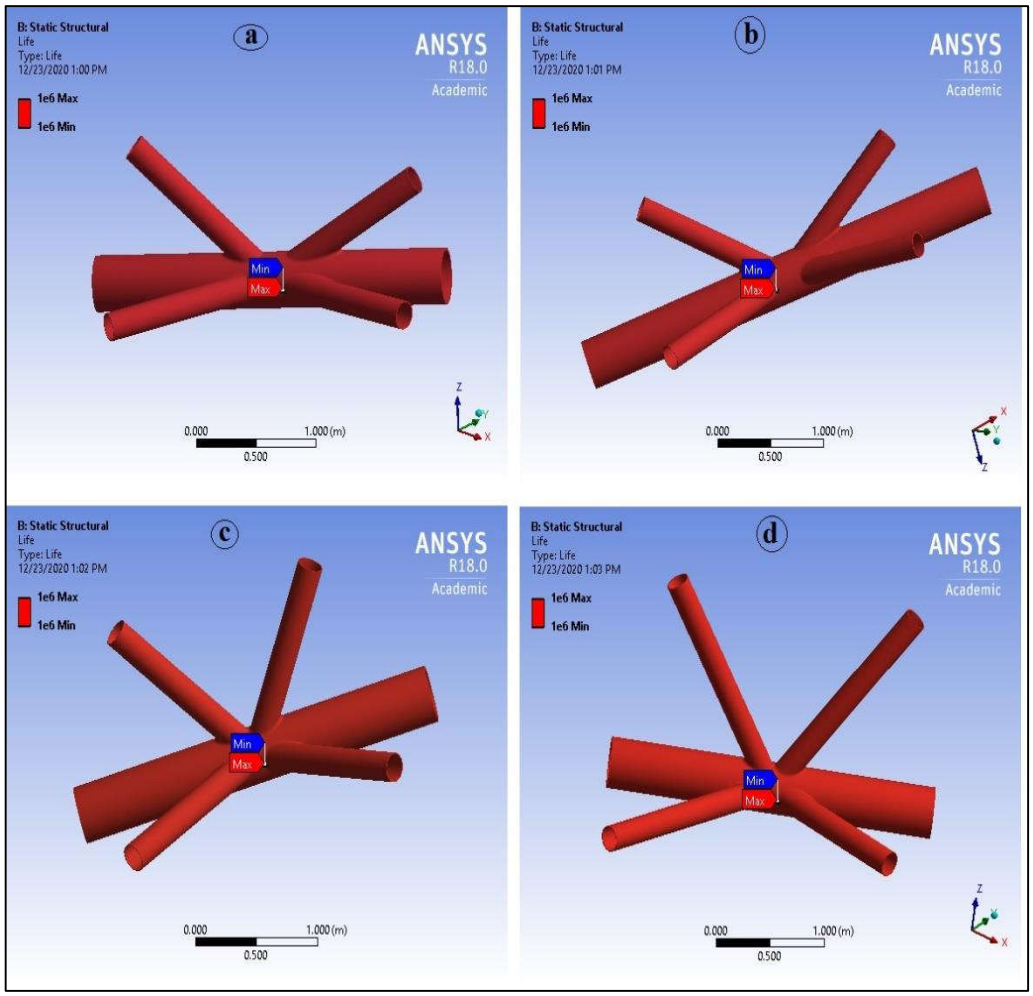

Figure 4.17 Fatigue life results for selected locations

The results of the observed value have been tabulated in table 4.17.

Table 4.17: Fatigue life results for critical joints

DYNAMIC ANALYSIS RESULTS FOR SELECTED JOINT LOCATIONS					
Load Case	**Type of result**	**Joint 1**	**Joint 2**	**Joint 3**	**Joint 4**

Boom swing to motion	Fatigue life (number of cycles)	1 x e6	1 x e6	1 x e6	1 x e6

d) Factor of safety

In this analysis, it has been found that the minimum value of factor of safety is 1.17 near the intersection point of brace and chord of joint 3 as shown in Figure 4.18. The points of maximum stress coincide with the lowest factor of safety with a value of 1.17. The rest of the joints under analysis have higher values of factor of safety. From the analysis it has also been correspondingly revealed that lowest factor of safety values has been attained under these conditions at joint 3.

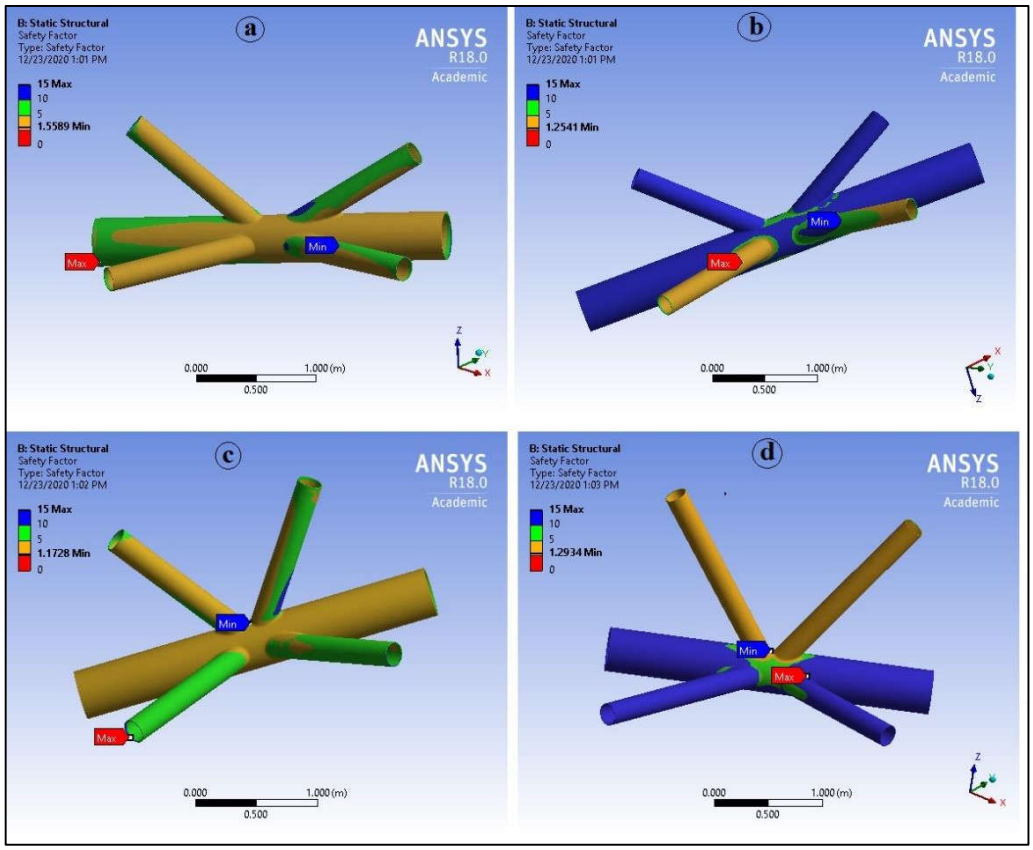

Figure 4.18 Factor of safety for selected joint locations

The results of the observed value have also been tabulated in table 4.18.

Table 4.18: Factor of safety results for critical joints

DYNAMIC ANALYSIS RESULTS FOR SELECTED JOINT LOCATIONS					
Load Case	**Type of result**	**Joint 1**	**Joint 2**	**Joint 3**	**Joint 4**
Boom swing to motion	Factor of safety	1.55	1.25	1.17	1.29

4.6.2 Boom swing-back phase with empty bucket

After the unloading of blasted rock to the disposal site, the dragline bucket swings back towards the blasted muck for again loading the bucket. Swing acceleration in the clockwise direction in this case rotates the upper machinery house along with boom to position the bucket for the next cycle of digging.

The computations of the swing velocity and acceleration have been explained in the research methodology chapter.

a) Global beam model results for dragline.

In the swing back phase of the dragline working cycle, the bucket remains empty and thus forces on the boom get reduced as shown in figure 4.19. The deformation value for the structure was therefore reduced up to 512 mm. Axial or direct stress values were obtained as 102.27 MPa in compression and 56.45 MPa in tension. Maximum bending stresses were obtained as 110.63 MPa at the point of attachment of rope connecting mast with boom point sheave.

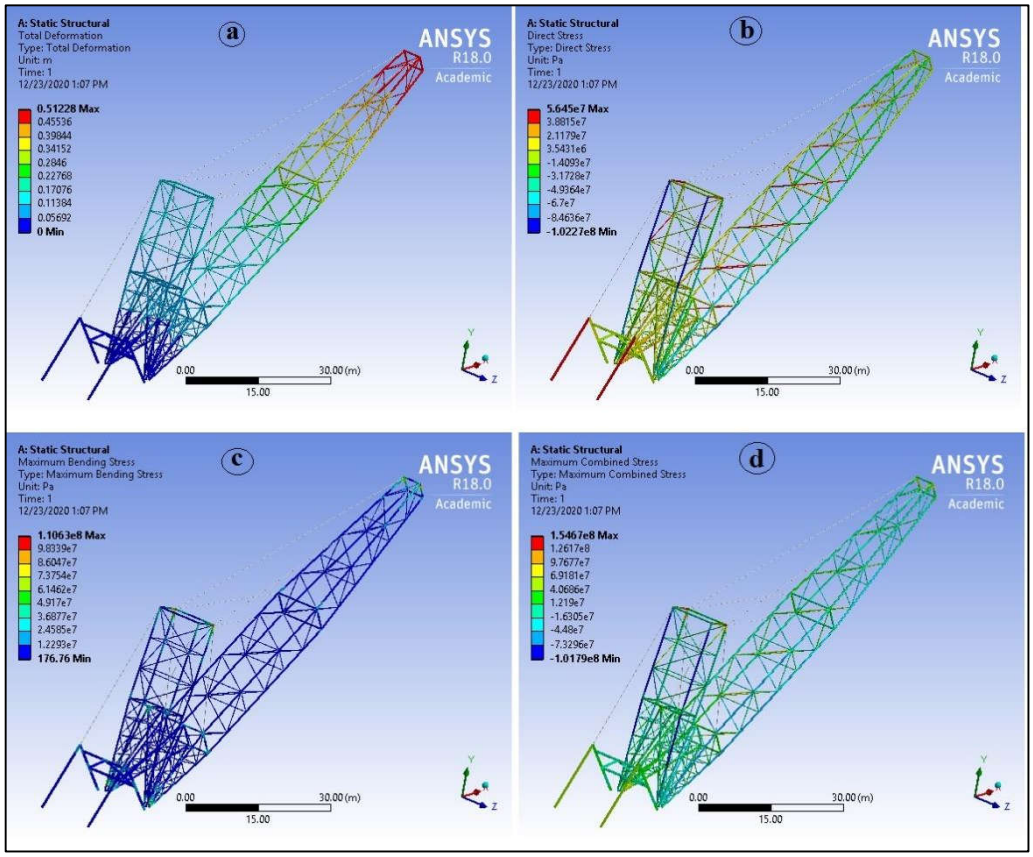

Figure 4.19 Global beam model results for a) deformation, b) axial stress c) maximum bending stress and d) maximum combined stress

The results of the observed value has been tabulated in table 4.19

Table 4.19: Results for global beam model

DYNAMIC ANALYSIS RESULTS FOR GLOBAL BEAM MODEL							
Load Case	**Deformation (m)**	**Direct Stress (MPa)**		**Maximum Bending Stress (MPa)**		**Combined Stress (MPa)**	
Boom swing back motion		Compression	102.27	Max.	110.63	Compression	101.79
	0.512						
		Tension	56.45	Min.	1.76 x e-4	Tension	154.67

b) Equivalent stress (Von-Mises) of dragline boom

The Von-Mises stress has been found as shown in figure 4.20 (a-d). Joint 4 has highest amount of stresses with a value of 123.38 MPa (figure 4.20 (d)). Equivalent stress for joint 1 was found to be 83.20 MPa, while stress value for joint 2 was 106.44 as depicted in figure 4.20 (a, b). The strategic location joint 3 was stressed at a stress level of 112.28 MPa (figure 4.20 (c).

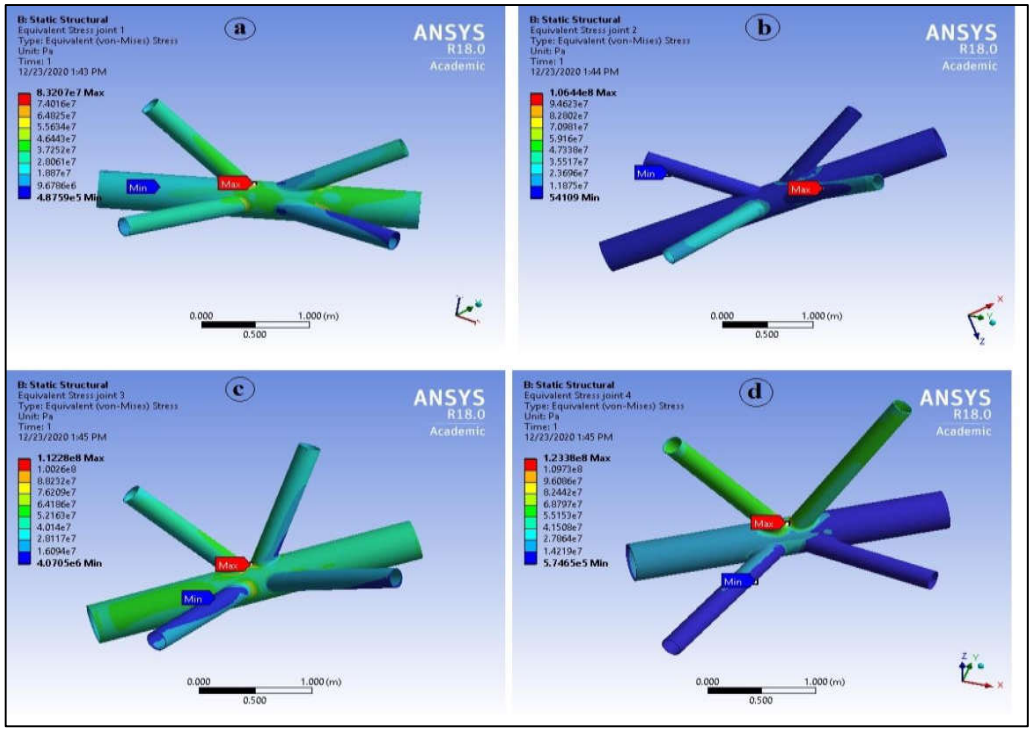

Figure 4.20 Equivalent stresses (Von-Mises) stress distribution for four selected joints

The results of the observed value have been tabulated in table 4.20.

Table 4.20 Equivalent stress results of critical joints

DYNAMIC ANALYSIS RESULTS FOR SELECTED JOINT LOCATIONS					
Load Case	**Type of result**	**Joint 1**	**Joint 2**	**Joint 3**	**Joint 4**
Boom swing back motion	Equivalent stress (MPa)	83.20	106.44	112.28	123.38

c) Fatigue life

Joints fatigue lives were computed as1xe^6 cycles as shown in figure 4.21 (a-d). It is clearly observed from Figure 4.21 that the stress magnitudes affect the fatigue life. The points subjected to high stress have low fatigue life and vice-versa. Furthermore, the fatigue strength is seriously reduced by the introduction of stress elevators such as, a notch or hole.

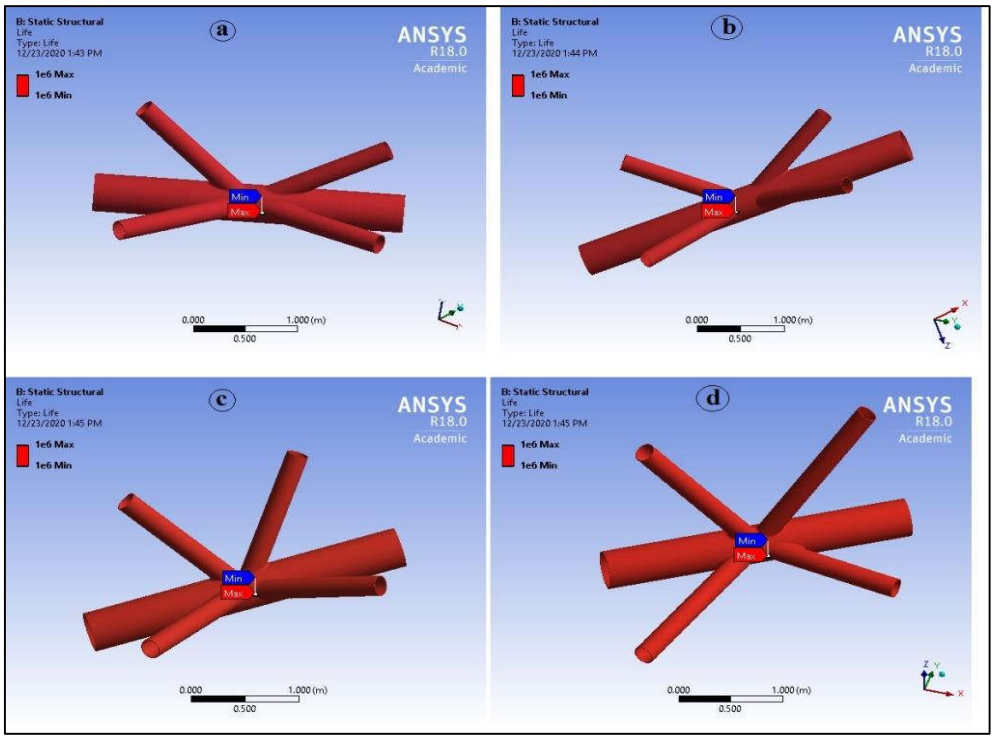

Figure 4.21 Fatigue life results for selected locations

The results of the observed value has been tabulated in table 4.21.

Table 4.21: Fatigue life results for critical joints

DYNAMIC ANALYSIS RESULTS FOR SELECTED JOINT LOCATIONS					
Load Case	**Type of result**	**Joint 1**	**Joint 2**	**Joint 3**	**Joint 4**
Boom swing back motion `	Fatigue life (number of cycles)	1 x e6	1 x e6	1 x e6	1 x e6

d) Factor of safety

In this analysis, it has been found that the minimum value of factor of safety is 1.35 near the intersection point of brace and chord of joint 4 as shown in figure 4.22. The rest of the joints under analysis have higher values of factor of safety. Again, it has been inferred that joint 3, which is near to the region of revolving center remains highly stressed. From the analysis it has been found that lower factor of safety values obtained under these conditions at joint 4. Joint 1 has the highest factor of safety of 2.00 due to the removal of external payload.

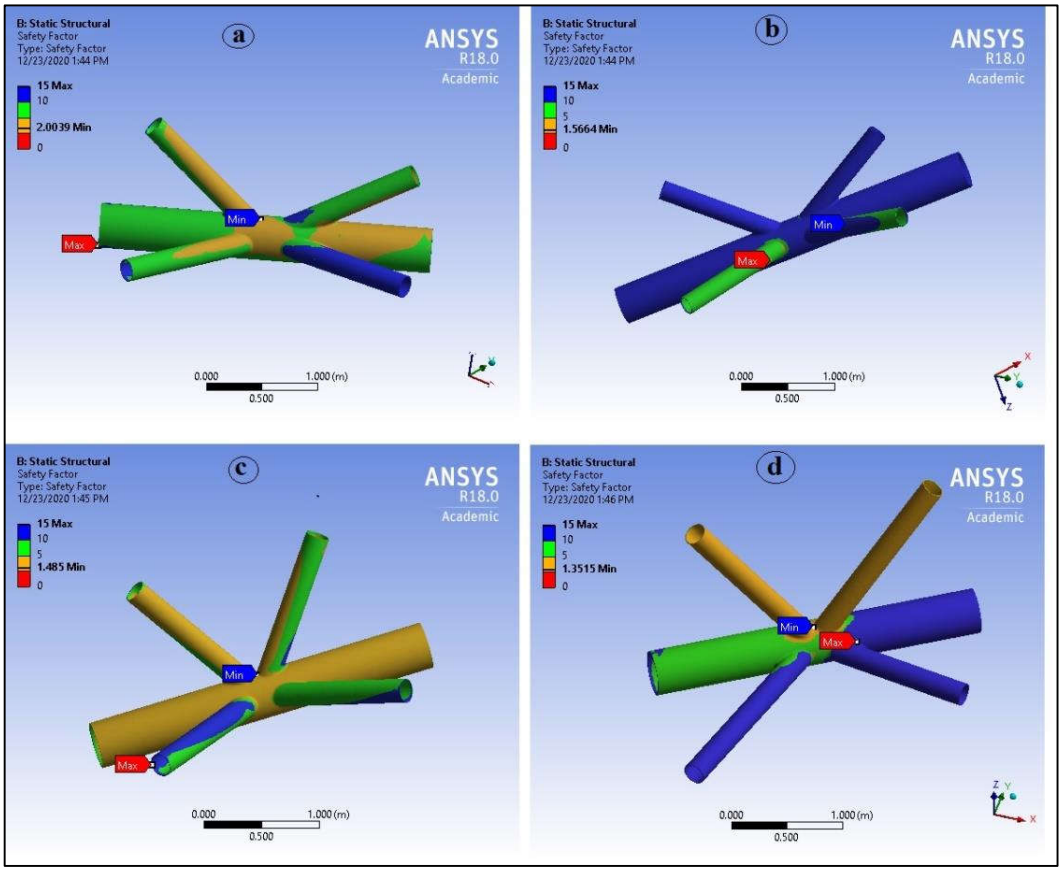

Figure 4.22 Factor of safety for selected joint locations

The results of the observed value have been tabulated in table 4.22.

Table 4.22: Factor of safety results for critical joints

DYNAMIC ANALYSIS RESULTS FOR SELECTED JOINT LOCATIONS					
Load Case	**Type of result**	**Joint 1**	**Joint 2**	**Joint 3**	**Joint 4**
Boom swing back motion `	Factor of safety	2.00	1.56	1.48	1.35

4.7 Summary for the dynamic loading case

Boom swing to motion is defined as the movement of dragline to an angular position required to dump the blasted material from digging to dumping site. While, swing back motion is expressed in terms of movement of dragline from dumping to digging site. During the swinging motion of the dragline, acceleration and retardation will affect the state of stresses on the boom structure. These values were assigned to the model and have been discussed in chapter 3.

Table 4.23 depicts the various results in the form of deformation, direct stresses, maximum bending stresses and combined stresses. Based on the observation it confirms that during the boom swing to motion the deformation and stresses are high as compared to swing back motion of dragline.

Table 4.23: Comparative dynamic analysis results for global beam model

DYNAMIC ANALYSIS RESULTS FOR GLOBAL BEAM MODEL							
Load Case	**Deformation (m)**	**Direct Stress (MPa)**		**Maximum Bending Stress (MPa)**		**Combined Stress (MPa)**	
Boom swing to motion		Compression	135.72	Max.	114.60	Compression	134.56
	0.683						
		Tension	76.26	Min.	1.76 x e-4	Tension	174.35
Boom swing back motion		Compression	102.27	Max.	110.63	Compression	101.79
	0.512						
		Tension	56.45	Min.	1.76 x e-4	Tension	154.67

Table 4.24: Comparative dynamic analysis results for solid sub-model

DYNAMIC ANALYSIS RESULTS FOR SELECTED JOINT LOCATIONS						
Load Case	**Sr. No.**	**Type of result**	**Joint 1**	**Joint 2**	**Joint 3**	**Joint 4**
Boom swing to motion	1.	Equivalent stress (MPa)	106.96	132.96	142.17	128.91
	2.	Fatigue life (number of cycles)	1 x e6	1 x e6	1 x e6	1 x e6
	3.	Factor of safety	1.55	1.25	1.17	1.29
Boom swing back motion `	1.	Equivalent stress (MPa)	83.20	106.44	112.28	123.38
	2.	Fatigue life (number of cycles)	1 x e6	1 x e6	1 x e6	1 x e6
	3.	Factor of safety	2.00	1.56	1.48	1.35

Based on analysis of overall structure of dragline illustrated above, the four joints location has been found critical. Table 4.24 gives the comparative result of the four study joint locations in terms of equivalent stress, fatigue life and factor of safety. In case of swing to motion results revealed that the stress in joint 3 is high as compared to other joints. The location of joint 3 and joint 4 is near to the revolving center of the dragline. It contributes higher stress effect on these joints as compared to the other joints. However, these stresses are not enough to significantly affect the fatigue life of the joints. Higher stress observed in joint 3 has seemingly reduced the factor of safety (1.17).

In case of swing back phase of dragline, the payload is removed therefore results in reduced value of stresses as compared to the stresses in swing to motion. Here, the stresses are found to be higher in joint 4 i.e. 123.38 MPa as compare to stresses in joint 3.

4.8 Results of Axial forces (tension) in wire ropes

As explained in research methodology chapter (section 3.12), the axial tensile forces on the suspension wire ropes have been critically analyzed after proper designing as illustrated in figure 3.18. The figure 3.18 clearly reveals the process of evaluating axial forces.

The axial forces have only been evaluated for the static loading case because lot of assumptions in the dynamic loading case increased the complexity and accuracy of the model. The table 4.25 summarizes the magnitudes of tension in all the suspension wire ropes of the dragline.

Table 4.25: Tensile axial forces in various wire ropes of dragline

Load cases	Suspension rope T_1 (KN)	Intermediate suspension rope-1 T_2 (KN)	Intermediate suspension rope-2 T_3 (KN)	Suspension rope A-frame T_4 (KN)
Self –weight of the boom	189.06	2001.51	458.62	300.01
Self-weight of boom ,along with tare weight of bucket	404.71	2699.23	567.16	305.37
Self-weight of boom ,along with bucket with payload	691.38	3629.30	701.81	311.15

The result of axial tensile forces T1, T2, T3 and T4 as observed in table 4.5 under various static loading conditions distinctly reveal that the forces are within the minimum breaking strength of the wire ropes the values for which are tabulated in table 4.25 itself within the brackets.

4.9 Results of Parametric study of boom clusters

The salient results of parametric variations for the safe design of critical joint 2 are discussed herewith reference to table 3.6 in research and methodology chapter.

4.9.1 Effect of change of chord diameter change

Four models were created to study the effect of chord diameter change on the resultant Von-Mises stresses. These four variations in the main chord diameter opted for the study and analysis were 406 mm, 390 mm, 350 mm and 300 mm respectively. All other parameters were kept unchanged. It is clear from the figure 4.23 that all other parameters were well within the design limit.

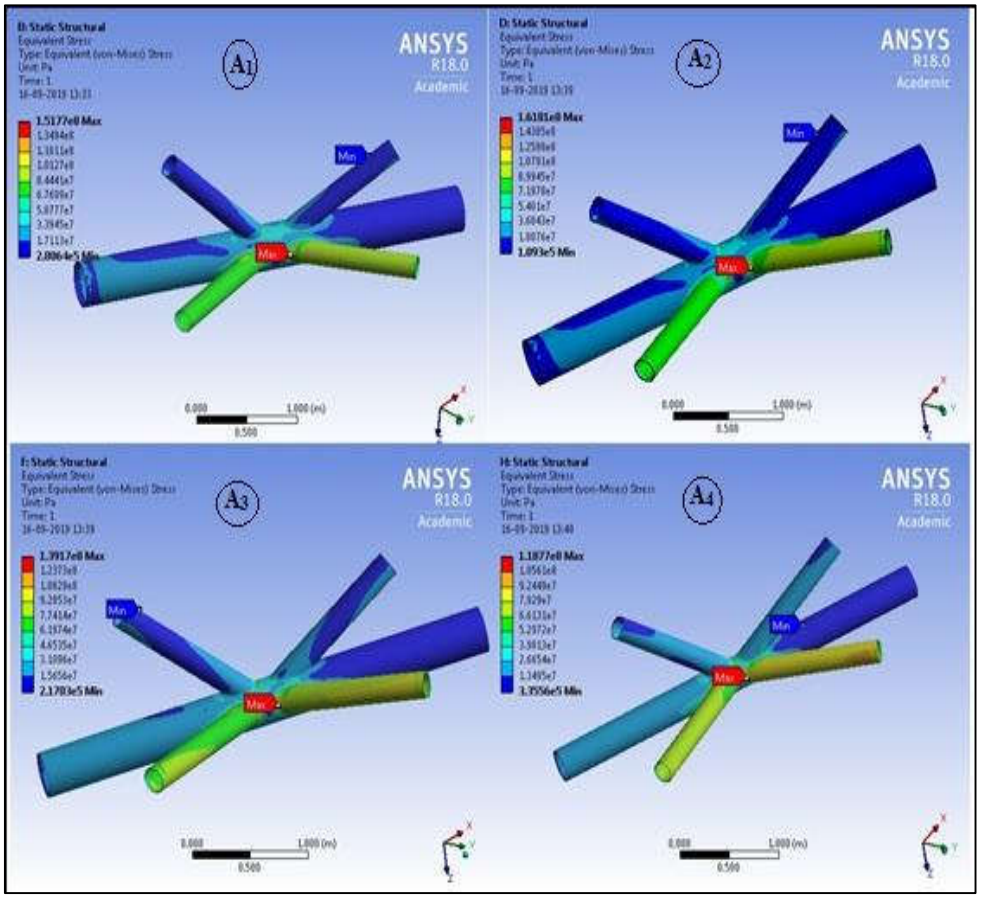

Figure 4.23 Main chord diameters of (a) 406 mm (b) 390 mm (c) 350 mm and (d) 300 mm

The stresses have been found within the yield strength of the material (250 MPa) under consideration. The equivalent Von-Mises stresses have been found to be minimum for the main chord diameter of 300 mm and maximum for the main chord diameter of 390 mm. It can be observed that as the main chord diameter decreases the stress values also decreases.

The results of the observed value have been tabulated in table 4.26.

Table 4.26: Effect of main chord diameter on stress value

Model No	d_0 (mm)	t_0 (mm)	d_i (mm)	t_i (mm)	β ratio (d/D)	γ ratio (Chord)	γ ratio (Brace)	Von-Mises Stress (MPa)
EFFECT OF MAIN CHORD DIAMETER ON STRESS VALUE								
A_1	406	20	207	8	0.50	10.15	12.9	151.70
A_2	390	20	207	8	0.53	9.75	12.9	161.80
A_3	350	20	207	8	0.59	8.75	12.9	139.10
A_4	300	20	207	8	0.69	7.50	12.9	118.70

4.9.2 Effect of change in chord thickness

To study the effect of change in value of Von-Mises stress due to the change in the thickness of chord, four models corresponding to the change in thickness of chord were designed and studied. The chord thicknesses of 20 mm, 16 mm, 12 mm and 8 mm were designed and studied. All other parameters were kept unchanged. The results of these changes are illustrated in the figure 4.24. The stress has been found within the yield strength of the material. The equivalent Von-Mises stress has been found to be minimum for the main chord thickness of 20 mm and maximum for the main chord thickness of 8 mm.

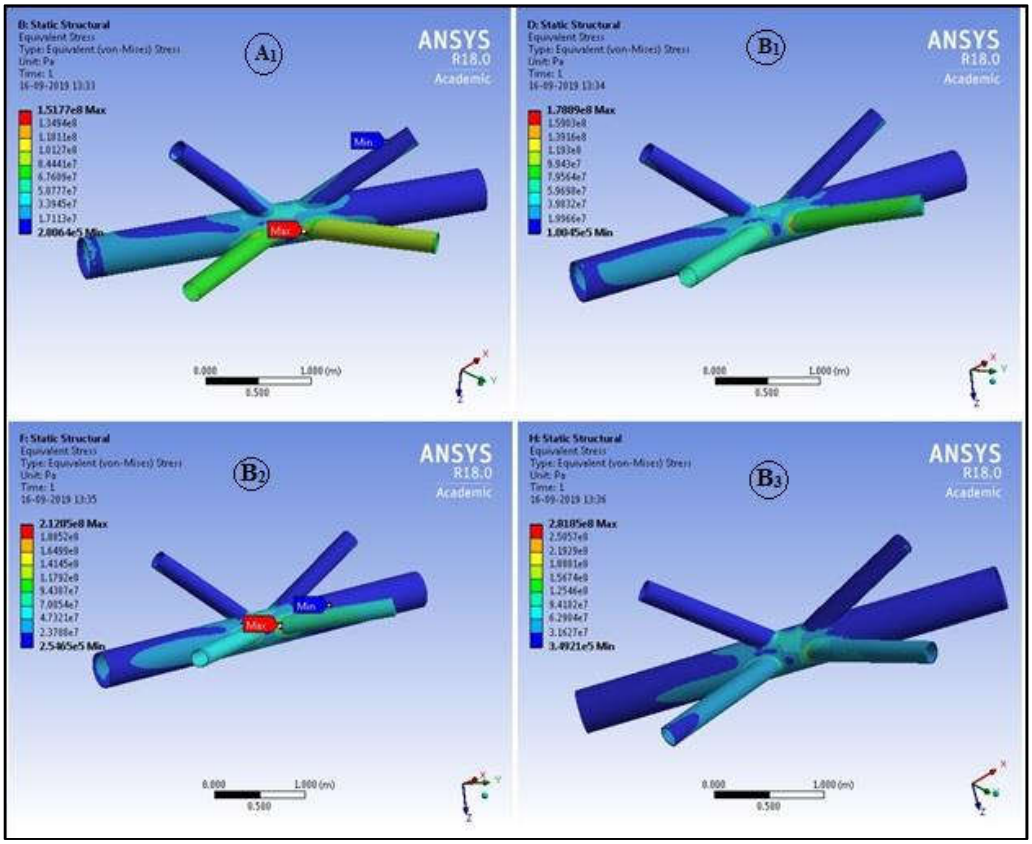

Figure 4.24 Main chord thicknesses of (a) 20 mm (b) 16 mm (c) 12 mm and (d) 8 mm

It can be observed that as the main chord thickness decreases the stress values increases as can be seen from figure 4.24 (a-d). The observations have been listed in table 4.27.

Table 4.27: Effect of change in main chord thickness

Model No	**d_0 (mm)**	**t_0 (mm)**	**d_i (mm)**	**t_i (mm)**	**β ratio (d/D)**	**γ ratio (Chord)**	**γ ratio (Brace)**	**Von-Mises Stress (MPa)**
EFFECT OF MAIN CHORD THICKNESSON STRESS VALUE								
A_1	406	20	207	8	0.50	10.15	12.9	151.70
B_1	406	16	207	8	0.50	12.68	12.9	178.89
B_2	406	12	207	8	0.50	16.91	12.9	212.05
B_3	406	8	207	8	0.50	25.37	12.9	281.85

4.9.3 Effect of change in the brace diameter

Brace diameter is another important parameter which governs the design and strength of hollow steel structure. Four changes were made in the brace diameter while keeping all other parameters unchanged. The four study models had brace dia. of 207 mm, 190 mm, 100 mm and 80 mm respectively. The results have been shown in figure 4.25. As the brace diameter decreases, the value of Von-Mises stress has been found to increase.

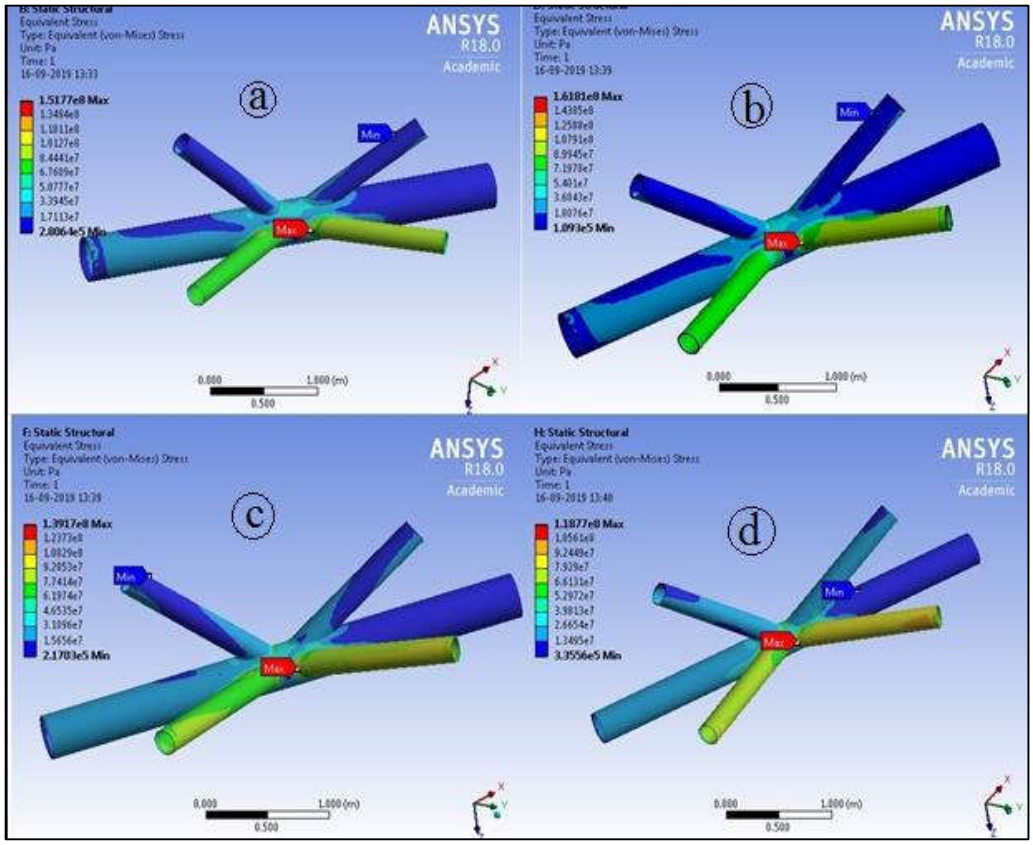

Figure 4.25 Equivalent stress results for brace diameters of (a) 207 mm (b) 190 mm (c) 100 mm and (d) 80 mm

This is due to local buckling of the brace that result in loss of the joint strength. A sudden spike in the value of Von-Mises stress has been observed for model with

brace diameter 80 mm as shown in the figure 4.25 (d). This is owing to the fact that this design did not follow the required criteria defined by CIDECT for β ratio, therefore very high value of stress has been observed (400.76 MPa). From this result, it can be inferred that if the design criteria violate the limits defined by CIDECT, the stresses would increase with decrease in fatigue life of structure.

The observed values has been tabulated in table 4.28.

Table 4.28: Effect of change in the brace diameter

Model No	d_0 (mm)	t_0 (mm)	d_i (mm)	t_i (mm)	β ratio (d/D)	γ ratio (Chord)	γ ratio (Brace)	Von-Mises Stress (MPa)
EFFECT OF BRACE DIAMETER ON STRESS VALUE								
A_1	406	20	207	8	0.50	10.15	12.9	151.70
C_1	406	20	190	8	0.46	10.15	11.87	173.94
C_2	406	20	100	8	0.24	10.15	6.25	351.41
C_3	406	20	80	8	0.19	10.15	5	400.76

4.9.4 Effect of change in brace thickness

Brace thickness affects the γ ratio as per the CIDECT design guidelines. The 3 different models were created along with the base design, which have the brace thickness of 8 mm. The thickness variation for the design b, c and d were 6 mm, 4 mm, and 2 mm respectively as revealed in figure 4.26 (a-d).

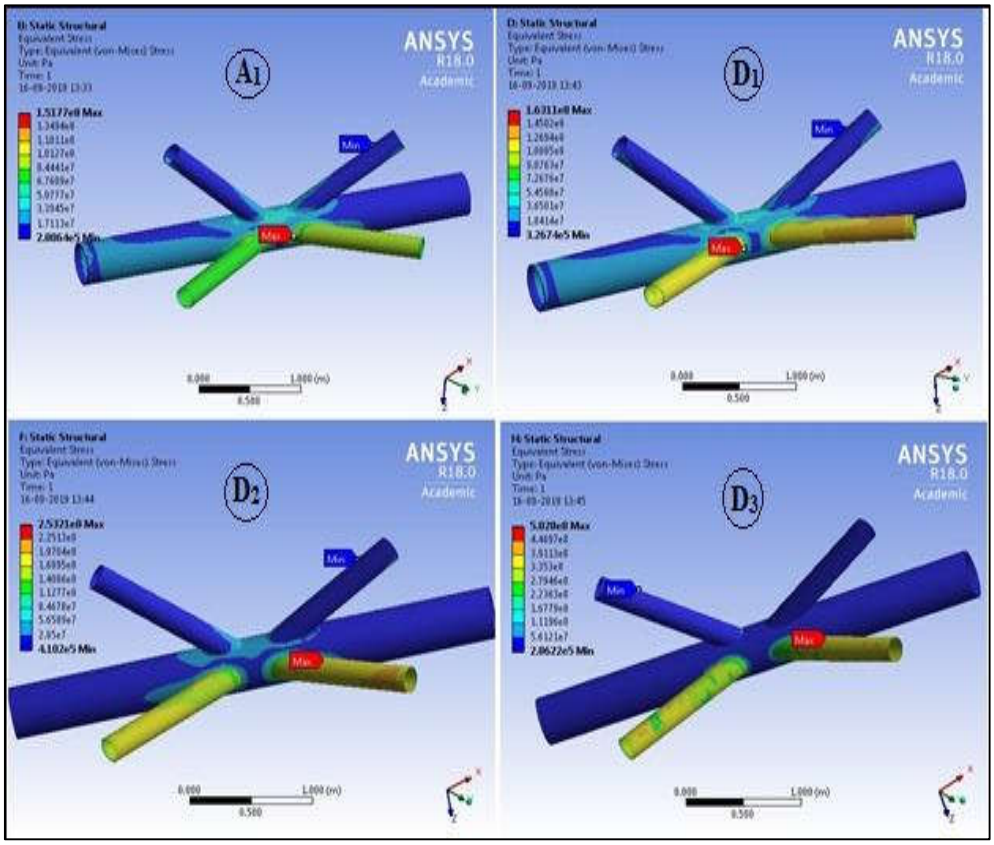

Figure 4.26 Equivalent stress results for brace thickness of (a) 8 mm (b) 6 mm (c) 4 mm and (d) 2 mm

The value of Von-Mises stress has been observed to increase with the decrease in value of brace thickness. The model with the thickness of 2 mm has been found to be highly stressed (502.8 MPa) as the γ ratio for this model was 51.75 which exceed the limiting value of 25. Also, the model with the brace thickness of 4 mm was found to be over stressed (up to 252 MPa), which is beyond the yield strength of the structural steel due to the γ ratio near to the limiting value 25. The other two models with brace thicknesses of 8 mm and 6 mm under consideration satisfy the γ ratio for the CHS

KK joint, and therefore, result in the lower stress value as compared to the models with brace thicknesses of 4 mm and 2 mm.

The observed values have been tabulated in table 4.29.

Table 4.29: Effect of change in brace thickness

Model No	d_0 (mm)	t_0 (mm)	d_i (mm)	t_i (mm)	β ratio (d/D)	γ ratio (Chord)	γ ratio (Brace)	Von-Mises Stress (MPa)
EFFECT OF BRACE THICKNESS ON STRESS VALUE								
A_1	406	20	207	8	0.50	10.15	12.9	151.70
D_1	406	20	207	6	0.50	10.15	17.25	163.11
D_2	406	20	207	4	0.50	10.15	25.87	253.21
D_3	406	20	207	2	0.50	10.15	51.75	502.80

4.10 Summary of parametric variation analysis

Table 4.30 below shows the equivalent stress (Von- Mises) results for the 13 models selected for the analysis. The variation in main chord diameter, main chord thickness, brace diameter, and brace thickness largely affect the stress value. These parameters are essential for design of a multiplaner circular hollow section (CHS) joint design**.**

Table 4.30: Results showing equivalent Stresses for parametric changes in the model

Model No	d_0 (mm)	t_0 (mm)	d_i (mm)	t_i (mm)	β ratio (d/D)	γ ratio (Chord)	γ ratio (Brace)	Von-Mises Stress (MPa)
EFFECT OF MAIN CHORD DIAMETER ON STRESS VALUE								
A_1	406	20	207	8	0.50	10.15	12.9	151.70
A_2	390	20	207	8	0.53	9.75	12.9	161.80
A_3	350	20	207	8	0.59	8.75	12.9	139.10
A_4	300	20	207	8	0.69	7.50	12.9	118.70
EFFECT OF MAIN CHORD THICKNESS ON STRESS VALUE								
A_1	406	20	207	8	0.50	10.15	12.9	151.70
B_1	406	16	207	8	0.50	12.68	12.9	178.89
B_2	406	12	207	8	0.50	16.91	12.9	212.05
B_3	406	8	207	8	0.50	25.37	12.9	281.85
EFFECT OF BRACE DIAMETER ON STRESS VALUE								
A_1	406	20	207	8	0.50	10.15	12.9	151.70
C_1	406	20	190	8	0.46	10.15	11.87	173.94
C_2	406	20	100	8	0.24	10.15	6.25	351.41
C_3	406	20	80	8	0.19	10.15	5	400.76
EFFECT OF BRACE THICKNESS ON STRESS VALUE								
A_1	406	20	207	8	0.50	10.15	12.9	151.70
D_1	406	20	207	6	0.50	10.15	17.25	163.11
D_2	406	20	207	4	0.50	10.15	25.87	253.21
D_3	406	20	207	2	0.50	10.15	51.75	502.80

The ratio obtained from these parameters must lie within the limit described by CIDECT for significant strength of the design. In the table, model B_3, C_2, C_3 and, D_3 have the stress values above the yield strength (250 MPa) of the material (structural steel). These models violate the design criteria in terms of $\boldsymbol{\beta}$ and $\boldsymbol{\gamma}$ ratio and hence resulted in very high stress values. Fatigue life is based on Von- Mises stress; therefore these high stress values significantly decrease the joint design life.

4.11 Verification of results

For verification of results on boom design and failure, some pictures of boom and joint failure have been used in the operating draglines in Indian coal mines.

Figure 4.27 (a) Boom failures in an Indian coal mine and, (b) location of crack within the boom cluster

Figure 4.27 (a) represents the failure of boom by bending under the dynamic loading condition while swinging back from the study field area. It depicts the collapse of boom structure under static loading condition while the bucket was being dragged

against the bank for filling. The location of failure for the dragline is at A-frame, which has been the location of maximum combined stress as found in the analysis.

Figure 4.27(b) indicates the location of crack within a cluster joint. The simulation results confirm the fact that stress is highly concentrated at the connecting nodes. The stress concentration on the chord side is lower than the stress concentrated on the brace side. The field maintenance logs also revealed that the brace members were meticulously replaced from time to time during the scheduled maintenance. The brace members failed due to fatigue at the welded area. Although the current work did not include the effect of different welding material to be used at the joints, yet the simulation outcomes provide sufficient insight about the weld failure by using fillet material in simulation studies, to represent the welding.